Synthesis and Pharmacological Evaluation of [^{11}C]granisetron and [^{18}F]fluoropalonosetron as PET Probes for 5-HT$_3$ Receptor Imaging

Linjing Mu,[†] Adrienne Müller Herde,[‡] Pascal M. Rüefli,[§] Filippo Sladojevich,[‡,#] Selena Milicevic Sephton,[‡,&] Stefanie D. Krämer,[‡] Andrew J. Thompson,[¶] Roger Schibli,[‡] Simon M. Ametamey,[‡] and Martin Lochner*[,§,⊥]

[†]Department of Nuclear Medicine, University Hospital Zürich, Rämistrasse 100, 8091 Zürich, Switzerland.

[‡]Center for Radiopharmaceutical Sciences of ETH, PSI and USZ, Vladimir-Prelog-Weg 4, 8093 Zürich, Switzerland.

[§]Department of Chemistry and Biochemistry, University of Bern, Freiestrasse 3, 3012 Bern, Switzerland.

[¶]Department of Pharmacology, University of Cambridge, Tennis Court Road, Cambridge CB2 1PD, UK.

Abstract

Serotonin-gated ionotropic 5-HT$_3$ receptors are the major pharmacological targets for antiemetic compounds. Furthermore, they have become a focus for the treatment of irritable bowel syndrome (IBS) and there is some evidence that pharmacological modulation of 5-HT$_3$ receptors might alleviate symptoms of other neurological disorders. Highly selective, high-affinity antagonists, such as granisetron (Kytril®) and palonosetron (Aloxi®), belong to a family of drugs (the 'setrons') that are well established for clinical use. To enable us to better understand the actions of these drugs *in vivo*, we report the synthesis of 8-fluoropalonosetron (**15**) that has a binding affinity (K_i = 0.26 ± 0.05 nM) similar to the parent drug (K_i = 0.21 ± 0.03 nM). We radiolabeled **15** by nucleophilic ^{18}F-fluorination of an unsymmetrical diaryliodonium

palonosetron precursor and achieved the radiosynthesis of 1-(methyl-^{11}C)-*N*-granisetron ([^{11}C]**2**) through *N*-alkylation with [^{11}C]CH_3I, respectively. Both compounds [^{18}F]**15** (chemical and radiochemical purity >95%, specific activity 41 GBq/μmol) and [^{11}C]**2** (chemical and radiochemical purity ≥99%, specific activity 170 GBq/μmol) were evaluated for their utility as PET probes. Using mouse and rat brain slices, *in vitro* autoradiography with both [^{18}F]**15** and [^{11}C]**2** revealed a heterogeneous and displaceable binding in cortical and hippocampal regions that are known to express 5-HT_3 receptors at significant levels. Subsequent PET experiments suggested that [^{18}F]**15** and [^{11}C]**2** are of limited utility for the PET imaging of brain 5-HT_3 receptors *in vivo*.

Key Words: 5-HT_3 receptor; positron emission tomography; granisetron; palonosetron; antagonist; imaging.

Introduction

Palonosetron (**1**, Aloxi®, Scheme 2) is a potent second generation 5-HT_3 receptor antagonist, and is the most recently approved drug for preventing acute (0 - 24 h) and delayed (24 - 120 h) emesis following moderate chemotherapy, with improved clinical efficacy when compared to early generation antagonists such as granisetron (**2**, Kytril®, Scheme 1).[1] *In vitro*, palonosetron also has a higher binding affinity for 5-HT_3 receptors (K_i = 40 pM) when compared to other antagonists (e.g. granisetron, K_i = 1.45 nM), and an extended *in vivo* plasma elimination half-life.[2-4] The reasons for these properties are not fully understood, but proposals have included unique allosteric effects, slow ligand dissociation and receptor internalization.[5,6]

5-HT_3 receptors belong to a family of receptors that also includes the γ-amino butyric acid ($GABA_A$), glycine and nicotinic acetylcholine (nACh) receptors. This is one of the largest families of ligand-gated ion channels and the receptors are responsible for fast synaptic neurotransmission in the central (CNS) and

peripheral nervous systems (PNS). All of the receptors are composed of five subunits that surround a central ion-conducting channel that spans the cell-surface membrane. Agonist activation of the receptor opens the central pore and allows ions to pass from one side of the membrane to the other, causing either depolarization or hyperpolarization. The subunits each contain three distinct structural regions termed the extracellular, transmembrane and intracellular domains. The extracellular domain is responsible for binding agonists that consequently leads to receptor activation. At the 5-HT_3 receptor, antagonistic drugs compete with serotonin (5-HT) at this orthosteric binding site and prevent the ion channel from opening. This action is responsible for alleviating the symptoms of nausea and vomiting.[1] Antiemetic activity is believed to involve both peripheral receptors and those in the CNS.[7-9] Several studies have also suggested that 5-HT_3 receptors are involved in neurological disorders, such as depression, drug abuse, schizophrenia, fibromyalgia, pruritus, bulimia nervosa and pain.[1,10-12]

Probes such as radioligands, antibodies and oligonucleotides have been used to map the distribution of 5-HT_3 receptors. First evidence of 5-HT_3 receptor expression in the rat brain came from binding studies using the selective 5-HT_3 receptor antagonist [^{3}H]GR65630.[13] These and other studies have consistently found that the highest levels of 5-HT_3 receptors in the CNS are located in the dorsal vagal complex in the brainstem, and in forebrain regions such as the hippocampus, amygdala, nucleus accumbens, putamen and caudate. The dorsal vagal complex includes the area postrema, nucleus tractus solitarius and the dorsal motor nucleus of the vagus nerve, regions that are responsible for the vomiting reflex.[8] Electrophysiology provides support for a predominantly presynaptic localization of these receptors, although some postsynaptic 5-HT_3 receptors are also reported.[14-17] Expression in other regions of the brain is usually low (see ref 18 for a comprehensive review). In the periphery, 5-HT_3 receptors are found in vagal afferent nerve fibers from the heart and GI tract which are responsible for the Bezold–Jarisch reflex and initiation of vomiting reflex, respectively.[19-21] 5-HT_3 receptors have also been found in ganglia of the myenteric plexus and submucosal plexus of the human intestine, consistent with their role in mediating gut contractions.[22-24] Elsewhere, lower densities of 5-HT_3 receptor can also be found on immune cells and tissues such as the

salivary glands.[25,26] Because of their wide tissue distribution, specific PET probes might be valuable for elucidating the role of 5-HT_3 receptors in associated disorders, although relating symptoms of such complex neuropsychiatric disorders to single neurobiological processes studied by PET can be challenging.[27]

To this end, the synthesis of several PET ligands that target the 5-HT_3 receptor were reported in the 1990s. For instance, 5-HT_3 receptor antagonists [^{11}C]MDL 72222,[28,29] [^{11}C]L-683877,[30] [^{11}C]Y-25130,[31] [^{11}C]YM060[31] and [^{11}C]KF17643[32] have been synthesized through *N*-alkylation with [^{11}C]CH_3I and their utility assessed in rodents and monkey. Similarly, the clinically-relevant antagonist **2** was ^{11}C-labeled at the bicyclic moiety yielding 9-(methyl-^{11}*C*)-granisetron[33] but to the best of our knowledge neither *in vitro* nor *in vivo* evaluation of this PET tracer was published. Other groups have radiolabeled the non-selective 5-HT_3 receptor agonist *N*-methylquipazine (NMQ, 2-(4-methylpiperazin-1-yl)quinoline), or partial agonists S21007 and MR18445, and evaluated the resulting tracers [^{11}C]NMQ,[34] [^{11}C]S21007[35,36] and [^{18}F]MR18445[37] in rat and monkey. However, all of these 5-HT_3 receptor PET probes were unsuitable as imaging agents, owing to high non-specific binding[28,29,32,34,36,37] or low brain uptake.[31] More recently, Zheng and colleagues have ^{11}C-labeled a series of benzoxazole partial 5-HT_3 receptor agonists[38] but no biological study with these PET tracers has been reported to date. While writing this manuscript, Mukherjee and colleagues also reported the synthesis of novel 5-HT_3 receptor ligand (*S*)-[^{18}F]fesetron, but found that the very low brain uptake in rats impairs its utility as a PET tracer.[39] Consequently, *in vivo* imaging of 5-HT_3 receptors in the CNS and PNS by PET remains to be accomplished.

Here, we report the synthesis of 1-(methyl-^{11}*C*)-*N*-granisetron ([^{11}C]**2**) and ^{18}F-labeled fluoropalonosetron ([^{18}F]**15**) and use these to characterize the distribution of 5-HT_3 receptors *in vitro* and *in vivo* in rodents.

Results and Discussion

Synthesis of 5-HT$_3$ Receptor Ligands and Precursors for Radiolabeling

The precursor **3** used for radiolabeling granisetron and unlabeled reference **2** were synthesized as shown in Scheme 1. Amide **3** was obtained in good yield following our previously published protocol[40] and subsequent selective *N*1-methylation was achieved by treatment with dimethyl carbonate and potassium carbonate in refluxing DMF.[41]

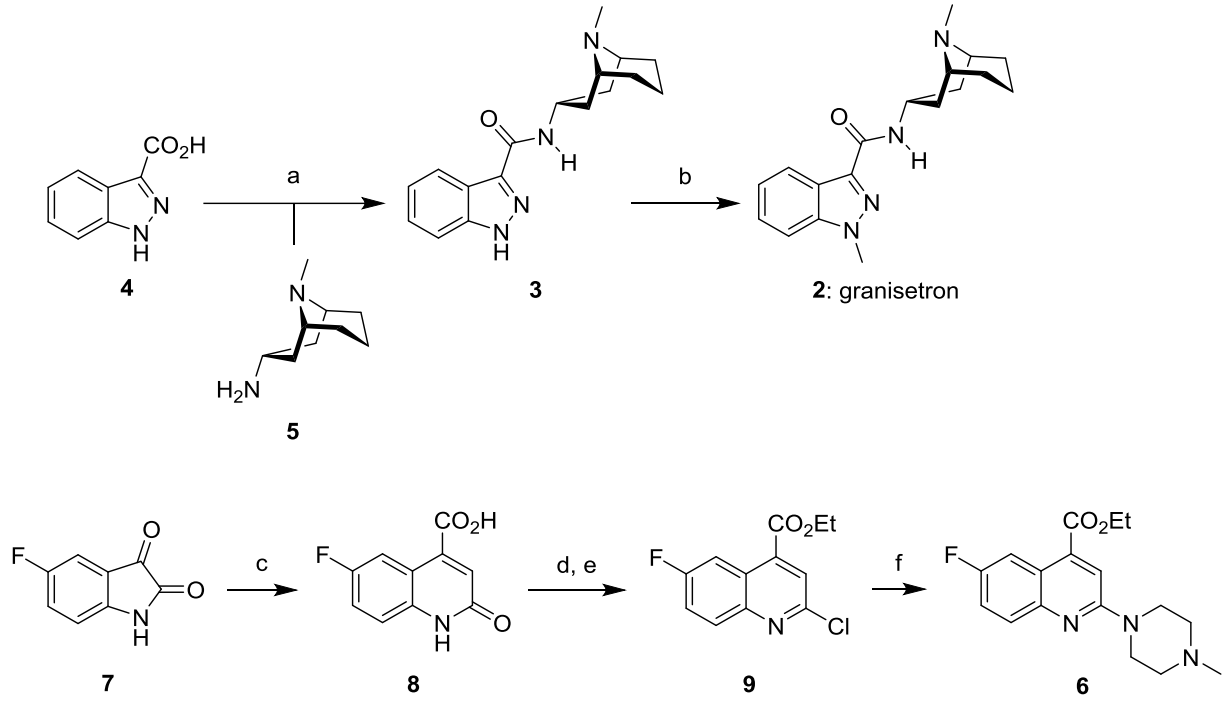

Scheme 1. Synthesis of non-labeled 5-HT$_3$ receptor ligands granisetron (**2**), quinoline-4-carboxylate **6**, and labeling precursor **3**. Reagents and conditions: (a) **5**, DCC, HOBt, CH_2Cl_2/DMF, rt, 73%. (b) K_2CO_3, dimethyl carbonate, DMF, reflux, 89%. (c) Ac_2O, reflux; NaOH, H_2O, reflux. (d) $POCl_3$, reflux, 98%. (e) $SOCl_2$, reflux; Et_3N, EtOH, rt, 89%. (f) 1-methylpiperazine, 140°C, 69%.

In a separate effort to develop novel 5-HT$_3$ receptor ligands based on NMQ, quinoline carboxylate **6** was discovered to bind with high affinity (K_i = 1.9 ± 1.0 nM) and compete for the same binding site as

[^{3}H]granisetron ([^{3}H]**2**).[42] We therefore decided to use structurally different **6** for blocking studies with the PET tracers (*vide infra*). It was synthesized starting from fluoroisatin **7** according to the route developed by Cappelli and colleagues for similar compounds (Scheme 1).[43] Briefly, **7** was ring-expanded via known Pfitzinger reaction to give oxoquinoline carboxylic acid **8**,[44] which was in turn chlorinated and esterified to yield 2-chloroquinoline carboxylate **9**. The piperazine substituent was subsequently introduced via S_NAr reaction and final quinoline carboxylate **6** was isolated in fairly good yield.

Palonosetron (**1**) was synthesized according to the published route,[45] with some minor experimental modifications (Scheme 2).

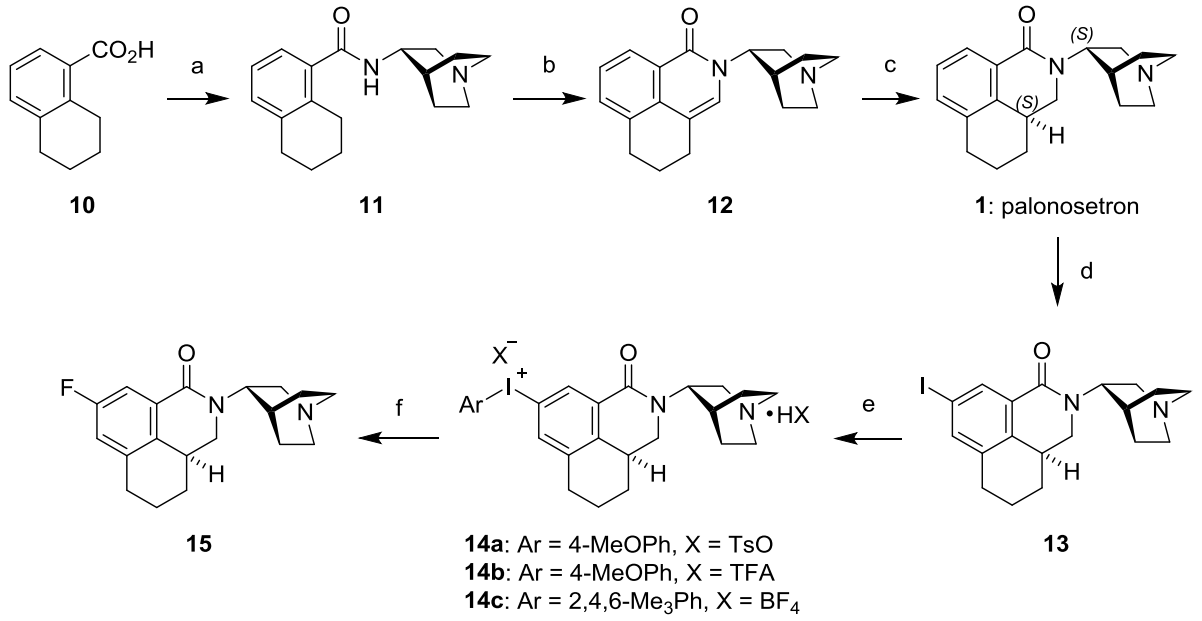

Scheme 2. Synthesis of reference compounds palonosetron (**1**), cold fluoropalonosetron **15**, and labeling precursors **14a-c**. Reagents and conditions: (a) (*S*)-3-Aminoquinuclidine hydrochloride, EDC, HOBt, *i*-Pr_2EtN, DMF, rt, 69%. (b) *n*-BuLi (2 equiv.), THF, -23°C; DMF, -23°C; HCl, H_2O, rt, 74%. (c) H_2 (25 bar), $Pd(OH)_2/C$ (20 mol%), $HClO_4$, HOAc, 70°C, 90%, *dr* 46:54; 4M HCl in dioxane/CH_2Cl_2; recrystallization from *i*-PrOH/H_2O, 27% (*S*,*S*)-**1**·HCl; sat. aq. $NaHCO_3$/EtOAc, 96% (d) NIS, CF_3SO_3H, rt, 41%. (e) *p*-TsOH·H_2O, mCPBA; anisole or mesitylene, CH_2Cl_2/TFE, rt; anion exchange, 23-67%. (f) Method A: **14a**, CsF, MeCN, 100°C, 14%. Method B: **14c**, $Cu(OTf)_2$, KF, 18-crown-6, DMF, 60°C, 13%.

Tetrahydronaphthalene carboxylic acid **10** was first coupled with chiral (*S*)-3-aminoquinuclidine mediated by EDC and HOBt in DMF. This procedure afforded amide **11** in much higher yields than the reported coupling via acid chloride, presumably due to the low solubility of the used quinuclidine hydrochloride in apolar organic solvents. Closure of the third ring to give isoquinolinone **12** was achieved by sequential lateral C-8 lithiation, formylation with DMF and intramolecular enamine formation. It is important to monitor the latter acid-mediated enamine formation and run it to completion, as too short reaction times will produce substantial amounts of cyclic hemiaminal (carbinolamine) which can be separated and dehydrated separately. The double bond character of the amide bond (lactam) in **12** imparts aromatic character to the ring system and hence the reduction of the enamine double bond requires fairly harsh conditions. In the event, high pressure of hydrogen in the presence of a palladium catalyst and strong acidic conditions at high temperature[45] reduced the double efficiently (90% yield) but with no diastereoselectivity (*dr* 46:54 (*S*,*S*)-**1**:(*R*,*S*)-**1**). In order to improve the diastereoselectivity in favor of the desired (*S*,*S*)-**1** isomer we briefly explored a more recent protocol published in a patent[46] (H_2 (10 bar), 20 mol% $Pd(OH)_2$/C, 58-62°C, EtOAc) that reported a higher diastereoselectivity (*dr* 6:4). However, in our hands, applying this procedure resulted in very slow conversion and no diastereoselectivity (*dr* 1:1). The two diastereomers of **1** were transformed into hydrochloride salts and separated by recrystallization which yielded pure (*S*,*S*)-**1** in moderate yield.

For the introduction of the ^{18}F-label we envisaged to use nucleophilic substitution of an unsymmetrical diaryliodonium salt of **1** with [^{18}F]fluoride.[47-52] To this end, we searched for methods to iodinate palonosetron (**1**). Direct iodination of non-activated aromatic rings is far less common than the corresponding chlorination or bromination. After exploring the few published protocols, the method described by Olah and co-workers, that utilizes *in situ* generated superelectrophilic iodine(I) trifluoromethanesulfonate,[53] worked best for us. This gave iodopalonosetron **13** as single regioisomer in acceptable yield. For the projected formation of diaryliodonium salts from **13** we initially employed the published one-pot procedures developed by Bielawski and Olofsson,[54] which was later refined by Zhu *et*

al..[55] We thought it more prudent to resort to a stepwise addition, as we found that **13** is readily overoxidized by excess oxidant (mCPBA), most probably to the corresponding *N*-oxide. In the reaction, mCPBA and *p*-toluenesulfonic acid were added to **13** and complete conversion to the corresponding bis-tosyloxyiodoaryl species **S1** (Scheme S1) was closely monitored by TLC, after which the aromatic compound was added to produce the *para*-substituted diaryliodonium salts **14** (for experimental details see *Methods*). Previous model studies indicate that nucleophilic fluorination of unsymmetrical diaryliodonium salts preferentially leads to ^{18}F-incorporation at the less electron-rich aromatic ring.[47] What is more, the counteranion of the diaryliodonium salt was found to significantly influence radiochemical yield (RCY).[56,57] Therefore, we chose to synthesize anisyl- and mesitylpalonosetron iodonium salts, in order to direct ^{18}F-fluorination towards the aromatic ring of palonosetron, and prepared **14a-c** with different counteranions. Isolation of pure and defined diaryliodonium salts is not trivial as handling of such compounds during workup and column chromatography leads to partial counterion exchange that is very difficult to analyze. Therefore, we utilized a reversed-phase HPLC ion-exchange protocol[57] to ensure generation of defined iodonium salts.

We used diaryliodonium salts **14** to access the standard reference fluoropalonosetron **15** for pharmacological characterization and confirming the identity of radiolabeled product by HPLC. To this end, anisylpalonosetron iodonium tosylate **14a** was heated in the presence of CsF in MeCN.[58] The fluorination reaction was very slow and did not go to completion after 51 h at 100°C, yet we were able to isolate pure **15** after preparative HPLC in low yield. Analysis of the reaction mixture by HPLC revealed that most of the starting diaryliodonium **14a** was either fluorinated at the anisole moiety (giving **13**) or thermally decomposed to palonosetron (product ratio **15**/**13**/**1** 20:39:41). With the aim of improving this product ratio and overall yield of **15** we also explored a copper(II) triflate-catalyzed fluorination reaction of **14c** with naked fluoride that relies on using the mesitylene-ring as dispensable aryl moiety.[59] Although we did observe complete disappearance of **14c** after 24 h at 60°C and obtained a much improved product ratio (**15**/**13**/**1** 60:13:27), isolation of pure **15** from this mixture by preparative HPLC proved difficult due to the structural similarity of the components.

The binding affinity of **15**, in competition with [^{3}H]granisetron ([^{3}H]**2**), was measured in HEK 293 cells stably expressing the human 5-HT$_3$A receptor and gave a K_i value of 0.26 ± 0.05 nM (n = 4), making **15** a promising candidate for PET imaging of 5-HT$_3$ receptors. The parent compound palonosetron (**1**) exhibited a similar binding affinity (K_i = 0.21 ± 0.03 nM, n = 5) in the same assay (Figure S1) and as reported elsewhere,[2] indicating that addition of a small fluorine atom did not significantly affect its binding affinity.

Radiolabeling

The radiosynthesis of 1-(methyl-^{11}*C*)-*N*-granisetron ([^{11}C]**2**) was achieved in a one-step procedure by *N*-methylation with [^{11}C]CH_3I in up to 30% RCY (decay corrected to EOB) (Scheme 3). The crude product was purified by semi-preparative HPLC and isolated in ≥99% radiochemical and chemical purity. The specific activity was in the range of 170 ± 26 GBq/μmol with a total activity of 3.1 ± 1.0 GBq at the end of the synthesis (n = 11). Overall, the radiosynthesis of [^{11}C]**2** took approximately 40 min from end of bombardment. For all *in vitro* and *in vivo* experiments [^{11}C]**2** was formulated in 5% ethanol in PBS buffer.

The diaryliodonium salts **14a-c** were ^{18}F-fluorinated using cesium [^{18}F]fluoride/kryptofix (K_{222}) complex in DMF in the presence of TEMPO (Scheme 3). The radiolabeling was performed in a homemade semi-automated, shielded hot-cell. Under the same reaction conditions, we found that both iodoanisole (**14a**, **14b**) and iodomesitylene (**14c**) leaving groups were displaced by [^{18}F]fluoride in the presence of Cs_2CO_3 and TEMPO in DMF at 140°C after 12 min. In our study, the anisyl iodonium salts (**14a** and **14b**) gave slightly higher RCYs than the mesityl iodonium salt (**14c**) (RCY 6% vs. 4%). For the anisyl iodonium salts, the influence of the counteranion on RCY was not significant (data not shown). Furthermore, presence of trace amounts of water in the solvent (DMF), as reported by others,[57,60] did not increase RCYs. Finally, using diaryliodonium precursor **14a**, [^{18}F]fluoropalonosetron ([^{18}F]**15**) could be synthesized and formulated for *in vivo* applications in approximately 6% RCY (decay corrected to EOB, n > 10) and with specific

activities at around 41 GBq/μmol at the end of the synthesis. We think that the rather low specific activity is probably due to the low radiolabeling yield. The radiochemical purity of [^{18}F]**15** was > 95% as determined by HPLC.

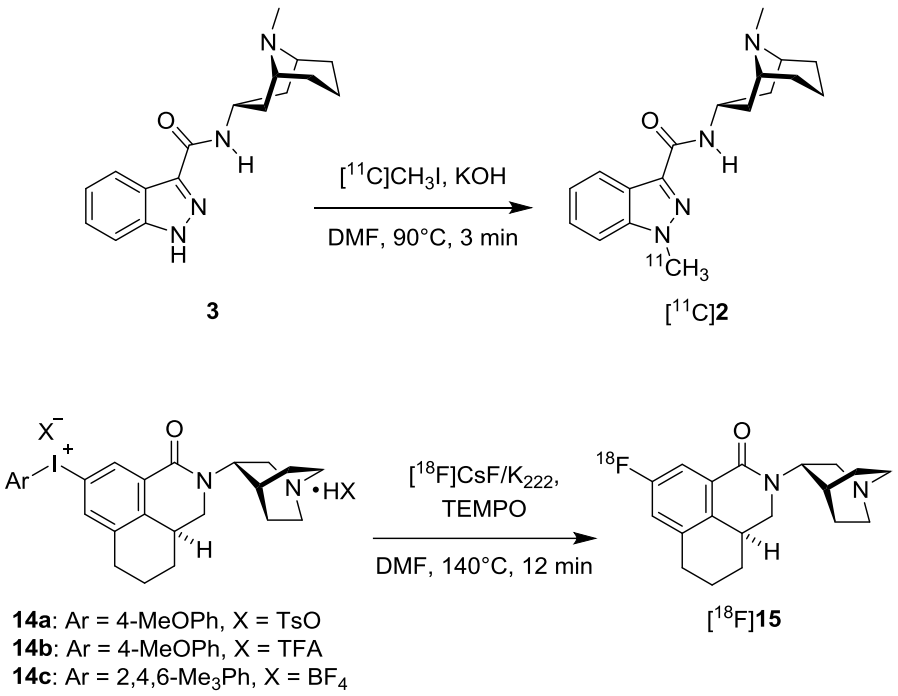

Scheme 3. Radiosynthesis of [^{11}C]**2** and [^{18}F]**15**.

When analyzing the [^{18}F]fluoride incorporation efficiency by RP-HPLC the influence of the pH of the mobile phase was very noticeable. For instance, in the case of the ^{18}F-fluorination reaction with precursor **14b** we measured 78% [^{18}F]fluoride incorporation by RP-HPLC when using 0.1% aq. TFA in the eluent (pH = 2). Analysis of the same reaction using 10 mM aq. NH_4HCO_3 buffer in the eluent (pH = 7.7) gave a significantly lower [^{18}F]fluoride incorporation value (< 3%). Similar observations were recently reported by Ory and colleagues who systematically studied the retention of [^{18}F]fluoride on different RP-HPLC columns that were eluted with mobile phases of different compositions and pH.[61] They observed increased [^{18}F]fluoride recovery with increasing pH. We reason that hydrogen fluoride (HF), due to its pK_a value of 3.19,[62] is almost completely dissociated at pH 5 and therefore the more polar [^{18}F]fluoride is not

retained on the RP-column. At pH 2, however, about 90% of [^{18}F]fluoride is present as [^{18}F]HF which may have stronger interactions with the silica core of RP-HPLC columns. Based on these observations, we would recommend to use an eluent with pH > 5 for silica based C18 RP-HPLC columns for both analytical and semi-preparative RP-HPLC of ^{18}F-labeled compounds.

In vitro Studies with [^{11}C]granisetron and [^{18}F]fluoropalonosetron

The stability of [^{11}C]**2** was assessed in rodent and human plasma over a period of 20 min during which no radioactive degradation products were detected (Figure S2). We determined a logD value of 0.43 ± 0.05 (n = 5) at physiological pH (7.4) for [^{11}C]**2** and of 0.93 ± 013 (n = 3) for [^{18}F]**15**. Both PET tracers have a basic tertiary amine in their bicyclic moiety and we believe the rather low logD values are likely to be due to protonation at physiological pH (calculated pK_a values for tertiary amines: 9.3 for **2** and 8.7 for **15**). The calculated lipophilicity (clogP) of the neutral species was 1.7 and 2.4, respectively.

Radiotracer binding was evaluated by *in vitro* autoradiography using mouse and rat brain slices as shown in Figure 1. Binding of [^{11}C]**2** was highest at hippocampus, cortical regions and septal area in both mouse and rat which is consistent with previous studies using other ^{11}C-labeled 5-HT$_3$ receptor ligands.[28,32,36] Binding of [^{11}C]**2** to these brain regions was specific as co-incubation with cold competitive ligands palonosetron (**1**, K_i = 0.21 ± 0.03 nM) or quinoline-4-carboxylate **6** (K_i = 1.9 ± 1.0 nM) completely diminished the radioactive signal (Figure 1A).

The binding of [^{18}F]**15** to mouse brain sections resulted in a heterogeneous radioactivity pattern with signals corresponding to hippocampal and cortical regions, and septal area. Blocking experiments using mouse brain slices that were co-incubated with [^{18}F]**15** and excess 5-HT$_3$ receptor competitive antagonists palonosetron (**1**) or quinoline-4-carboxylate **6** resulted in complete loss of all these signals (Figure 1B, top panels). In rat brain sections incubated with [^{18}F]**15**, high signal intensity was observed in hippocampal regions, which was almost completely abolished by blocking conditions with cold **1** or **6** (Figure 1B, bottom

panels) indicating specific binding. This is in line with recent findings where *ex vivo* microPET images of whole rat brain also showed strong hippocampal staining with the palonosetron congener (*S*)-[^{18}F]fesetron.[39] Specific binding to hippocampus was also observed with high affinity 5-HT$_3$ antagonist [^{3}H]GR65630 (B_{max} 4.9 ± 0.6 and 1.3 ± 0.3 fmol/mg protein for rat and mouse, respectively).[63]

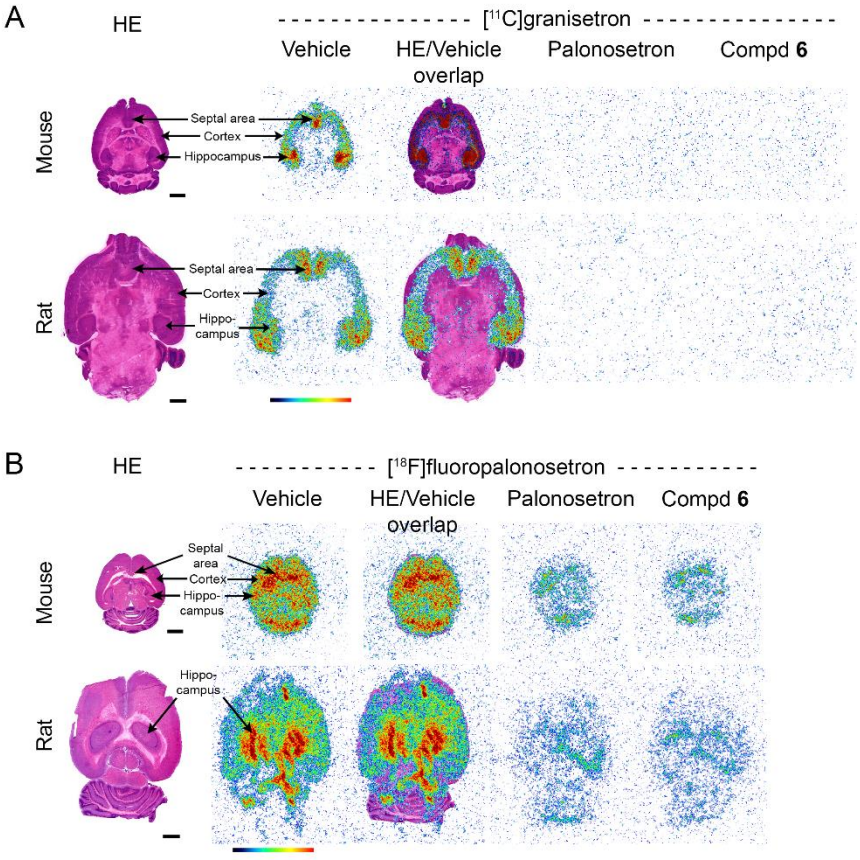

Figure 1. Representative autoradiography images of coronal mouse or rat brain sections after incubation with (A) [^{11}C]granisetron ([^{11}C]**2**, 0.6 nM) or (B) [^{18}F]fluoropalonosetron ([^{18}F]**15**, 0.4 nM) under baseline (vehicle) or blocking conditions (co-incubation with palonosetron (**1**, 1 μM) or quinoline-4-carboxylate **6** (1 μM)). Autoradiograms are superimposed onto morphological hematoxylin-eosin (HE)-stained slices with a color scale for low (blue) to high (red) binding. Identification of specific brain regions was based on HE staining and according to the anatomical atlas.[64] Scale bars: 2 mm.

We attribute the different radioactive labeling patterns of [^{11}C]**2** and [^{18}F]**15** to the difference of mouse and rat brain sections, as indicated by hematoxylin-eosin (HE) staining, as well as their difference in chemical structures and specific radioactivities (137-189 GBq/μmol and 41 GBq/μmol, respectively). The specific labeling of distinct rodent brain-regions (e.g. hippocampus, cortical regions, septal area) encouraged us to evaluate both [^{11}C]**2** and [^{18}F]**15** as PET tracers in *in vivo* experiments.

In vivo Studies using [^{11}C]granisetron and [^{18}F]fluoropalonosetron

In vivo brain-PET scans were performed in rats to study the uptake of [^{11}C]**2** and [^{18}F]**15** under baseline and blocking conditions with palonosetron (**1**). For both tracers, we found very low and homogeneous radiotracer accumulation in the brain (Figure 2A). Further, from these PET scans, we calculated the time-activity curves (TACs, Figure 2B) for the brain regions that have been previously identified to contain 5-HT$_3$ receptors.[13] Specifically, this earlier study used high-affinity antagonist [^{3}H]GR65630 on rat brain homogenates which gave the highest specific binding in the entorhinal cortex and area postrema, the latter of which is known to control vomiting. In the MRI-template implemented in our biomedical imaging software, the area postrema it is part of the medulla oblongata. No specific binding of either [^{11}C]**2** or [^{18}F]**15** to the aforementioned brain region was detected (Figure 2B). Furthermore, while the most intense signal was observed in the pituitary gland, uptake of [^{11}C]**2** and [^{18}F]**15** was not blocked by **1** and indicates that the signal was non-specific. In line with our findings, low brain uptake and strong non-specific accumulation of activity in pituitary gland was reported in a recent SPECT imaging study of the serotoninergic system in rat (targeting 5-HT$_{1A}$, 5-HT$_{2A}$ and 5-HT$_4$ receptors, and serotonin transporter SERT).[65] The absence of specific binding of our 5-HT$_3$ receptor radioligands might be due to the low receptor number (B_{max}), which was reported to be 1-11 fmol/mg protein in rat and mouse brain when using high-affinity 5-HT$_3$ receptor antagonist [^{3}H]GR65630.[63,66] Such low B_{max} values make brain 5-HT$_3$ receptors a highly challenging target for PET imaging. Furthermore, the partition coefficients (logD) of

both [^{11}C]**2** and [^{18}F]**15** are lower than the optimal average lipophilicity value of 2.1 for brain penetrating compounds.[67]

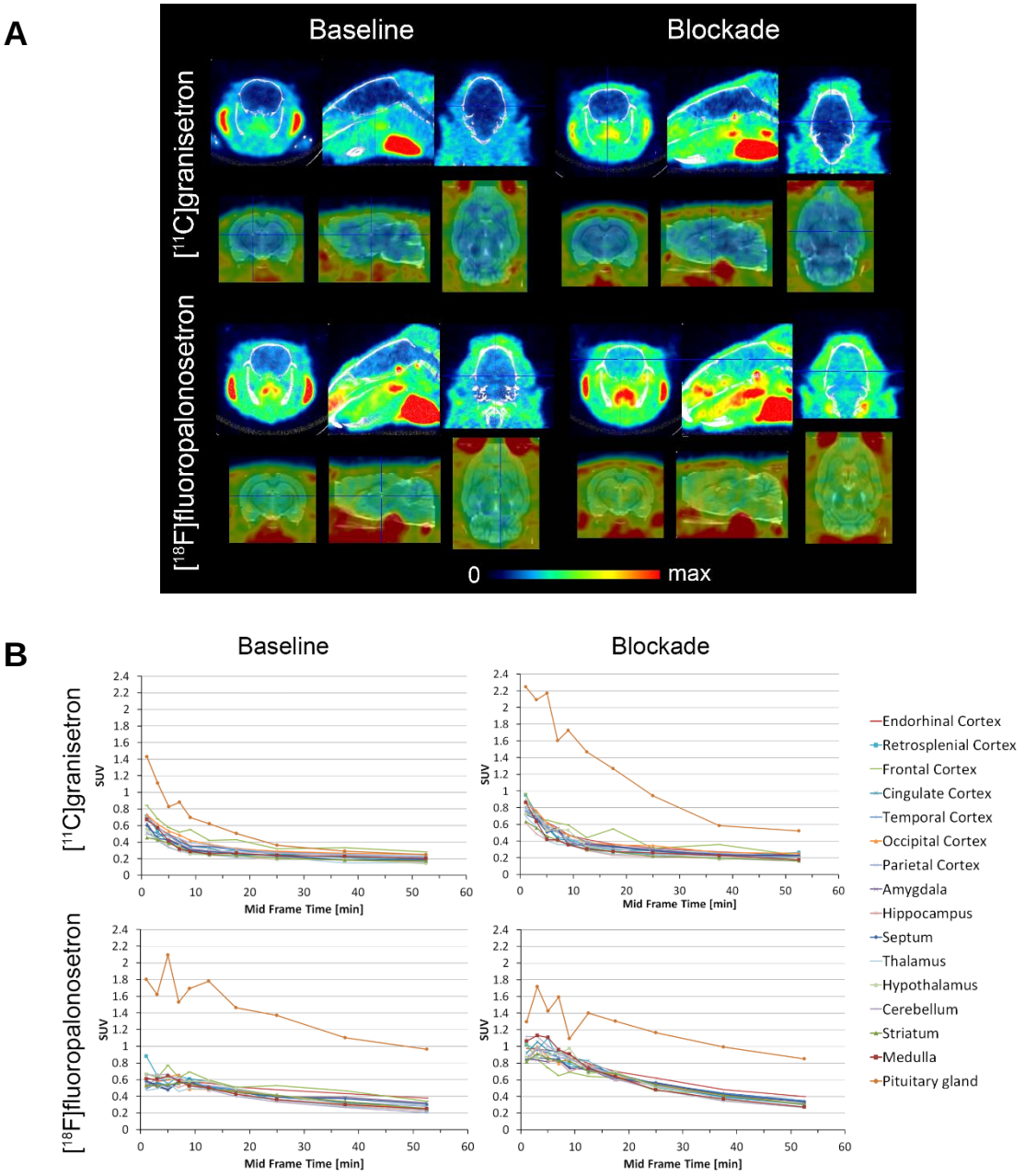

Figure 2. (A) PET brain images of Wistar rats using [^{11}C]granisetron ([^{11}C]**2**, top panels) or [^{18}F]fluoropalonosetron ([^{18}F]**15**, bottom panels) under baseline or blocking conditions (100 μg/kg **1**). Images are averaged 0-60 min post-radiotracer injection and superimposed on an MRI template, showing axial, sagittal and coronal sections (from left to right). SUV_{max} = 1.5 (PET/CT images) or 0.8 (PET/MRI

images). (B) TACs of selected rat brain regions obtained with [^{11}C]**2** (top graphs) or [^{18}F]**15** (bottom graphs) under baseline or blocking conditions. TACs were generated from the same rats as shown in (A).

5-HT$_3$ receptors are not only expressed in the CNS but also in the periphery, most prominently on enterochromaffin cells of the GI tract. Body-PET scans of rats using either [^{11}C]**2** or [^{18}F]**15** revealed significant uptake in liver and intestines for both tracers (Figure 3). At late time points, uptake in stomach wall was also observed, in particular for [^{18}F]**15**. Furthermore, we found marked accumulation of [^{18}F]**15** in lungs within the first few minutes after injection. This is similar to other reports where an accumulation of PET signal in this organ was detected with ^{11}C-labeled 5-HT$_3$ receptor antagonists [^{11}C]MDL 72222,[28] [^{11}C]Y-25130,[31] [^{11}C]YM060[31] and [^{11}C]KF17643[32] in rodents.

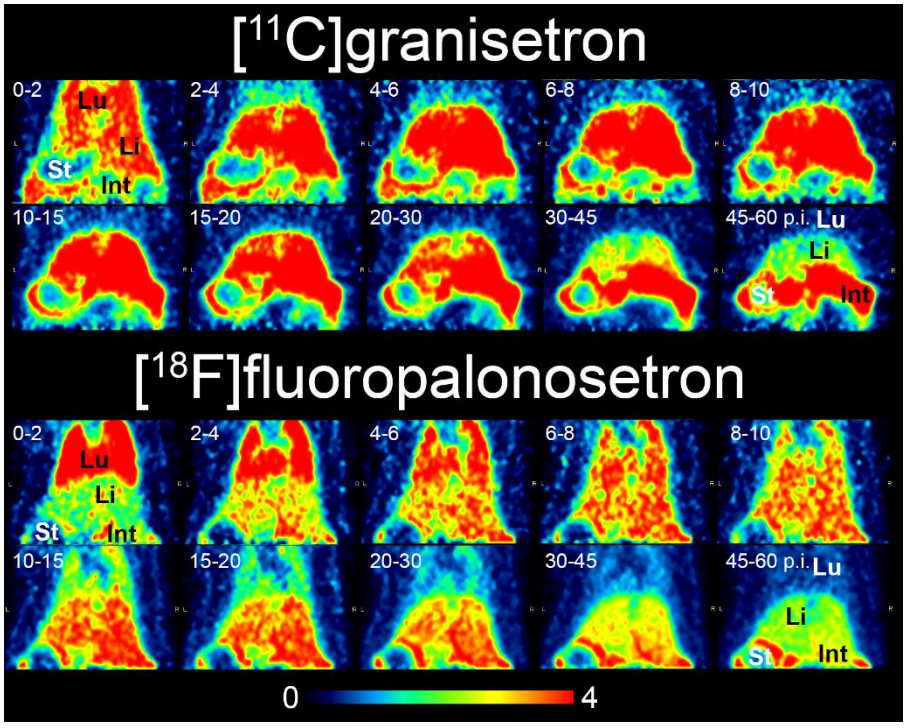

Figure 3. Coronal PET images of [^{11}C]granisetron ([^{11}C]**2**, top panels) or [^{18}F]fluoropalonosetron ([^{18}F]**15**, bottom panels) in the lung-liver-intestine region in rat. Time series images averaged over the indicated time (in min) post-injection (p.i.). Labels: Lu, lung; Li, liver; St, stomach; Int, intestine.

Conclusions

We have successfully synthesized and radiolabeled the clinically-relevant 5-HT_3 receptor antagonists granisetron (**2**) and palonosetron (**1**). *In vitro* autoradiography using 1-(methyl-^{11}C)-*N*-granisetron ([^{11}C]**2**) and [^{18}F]fluoropalonosetron ([^{18}F]**15**) showed specific labeling in rodent brain slices that were consistent with a previous study that used tritiated 5-HT_3 receptor antagonist [^{3}H]GR65630.[13] We found that *in vivo* PET studies in rats gave low and homogenous radiotracer signals of [^{11}C]**2** and [^{18}F]**15** in brain. We speculate that this might be due to 1) the low expression of 5-HT_3 receptors in brain (B_{max} 1-11 fmol/mg protein) and 2) the basic tertiary amino groups of [^{11}C]**2** and [^{18}F]**15** that in turn leads to 3) low $logD_{7.4}$ values for both tracers which is at the lower end of the optimal range (0-3) for passing through the blood-brain barrier. Although **1** and **2** are very efficient drugs, we conclude that [^{11}C]**2** and [^{18}F]**15** are not suitable radioligands for *in vivo* PET imaging of 5-HT_3 receptors in rodents, and in general, developing specific, high-brain uptake 5-HT_3 receptor PET tracers remains a challenge.

Methods

General Chemistry. All reagents and solvents were purchased from Sigma-Aldrich Chemie GmbH (Germany), Merck (Germany), Acros (Belgium), ABCR GmbH (Germany) or Fluka (Switzerland). All chemicals were used as supplied without further purification, except mCPBA which was dried at high vacuum for at least 1 h before use. Anhydrous solvents were obtained by filtration through dry alumina columns under argon pressure. Synthesized compounds were >95% in purity determined by analytical HPLC method on an Agilent HPLC system. Reactions were monitored by TLC on 0.2 mm ALUGRAM Xtra SIL G/UV or POLYRAM Alox N/UV plates (Machery-Nagel). Flash column chromatography was carried out using Fluka analytical 60752 silica gel (pore size 60 Å, 40-63 μm particle size) or CAMAG 507-C neutral aluminum oxide (pore size 60 Å, 40-160 μm particle size). Infrared (IR) spectra were recorded on a Jasco FT-IR-460 Plus. NMR spectra were recorded on a Bruker Avance 300 (^{1}H at 300 MHz,

^{13}C at 75 MHz) and Avance II 400 (^{1}H at 400 MHz, ^{13}C at 100 MHz, ^{19}F at 376 MHz). Chemical shifts (δ) are reported in ppm referenced to the residual solvent peak. Multiplicities: s = singlet, d = doublet, t = triplet, q = quartet, m = multiplet, br = broad peak. Coupling constants (*J*) are reported in Hz. High resolution mass spectrometry (HRMS) was performed on a Thermo Scientific LTQ Orbitrap XL with a Nanospray Ionsource. For purification of radiolabeled product, a semi-preparative Merck-Hitachi L2130 HPLC system equipped with a radiation detector VRM 202 (Veenstra Instrument, Joure, Netherlands) was used with a Waters Symmetry C8 Prep Column (50 x 7.8 mm, 100 Å, 5 µm) and a gradient method: 10 mM ammonium bicarbonate buffer (solvent A) and CH_3CN (solvent B) 0.0-1.0 min 5% B; 1.0-12.0 min, 5-50% B; 13.0-20.0 min, 50% B; 20.0-20.1 min, 50-5% B; 20.1-40.0 min, 5% B at a flow rate of 4 mL/min. For product analysis, an analytical Agilent 1100 series HPLC system, equipped with UV multi-wavelength detector and a GabiStar radiodetector (Raytest) was used with an ACE C18-AR column (50 x 4.6 mm, 3 µm) with the following conditions: 0.1% TFA in H_2O (solvent A) or 10 mM ammonium bicarbonate buffer (solvent A), CH_3CN (solvent B); 0.0-8.0 min, 5-50% B; 8.0-9.0 min, 50% B; 9.0-9.1 min, 50-5% B; 9.1-12.0 min, 5% B at a flow rate of 1 mL/min.

For the preparation of reference compound **2** and blocker compound **6** see the *Supporting Information.* Labeling precursor **3** was synthesized as published elsewhere.[40]

***N*-((1*R*,3*S*,4*R*)-Quinuclidin-3-yl)-5,6,7,8-tetrahydronaphthalene-1-carboxamide (11).** We have modified the previously reported synthesis[45] of this compound. To a suspension of 5,6,7,8-tetrahydronaphthalene-1-carboxylic acid (**10**, 3.98 g, 22.6 mmol), (*S*)-3-aminoquinuclidine dihydrochloride (3.00 g, 15 mmol) and HOBt monohydrate (3.46 g, 22.6 mmol) in 35 mL DMF, was added DIPEA (10.5 mL, 60 mmol) and EDC (5 mL, 28.7 mmol). The reaction mixture was stirred at rt for 27 h and the reaction quenched by the addition of 100 mL 5M NaOH solution. The water phase was extracted EtOAc (3 x 150 mL), the combined organic layers were washed with 350 mL of 2M NaOH, dried over Na_2SO_4, filtered and concentrated under reduced pressure to afford a yellow oil. EtOAc (70 mL) was added and the organic phase was washed again with 2M NaOH (2 x 70 mL), concentrated and the resulting residue co-evaporated

with CH_2Cl_2 (2 x 20 mL), giving an oily foamy solid (5.33 g). The crude product was purified by flash chromatography on silica gel, using CH_2Cl_2/MeOH /Et_3N 9:1:0.1, to afford a white foamy solid (3.64 g). In order to remove Et_3N-contaminations, the compound obtained after flash chromatography was partitioned between 100 mL CH_2Cl_2 and 100 mL sat. aq. $NaHCO_3$ solution. The water phase was extracted with CH_2Cl_2 (2 x 100 mL). The combined organic layers were dried over Na_2SO_4 and concentrated to yield **11** as a white foamy solid (2.95 g, 69%). ^{1}H NMR (300 MHz, DMSO-*d6*) δ 8.26 (d, *J* = 6.9, 1H), 7.17 – 7.01 (m, 3H), 3.98 – 3.81 (m, 1H), 3.08 (ddd, *J* = 13.4, 9.7, 2.0, 1H), 2.86 – 2.63 (m, 8H), 2.57 (dd, *J* = 14.2, 5.5, 1H), 1.86 (dd, *J* = 6.1, 3.0, 1H), 1.79 – 1.66 (m, 5H), 1.63 – 1.50 (m, 2H), 1.36 – 1.27 (m, 1H). HRMS (ESI+) calcd for $C_{18}H_{25}N_2O$ $[M+H]^+$ 285.1960, found 285.1963.

2-((1*R*,3*S*,4*R*)-Quinuclidin-3-yl)-2,4,5,6-tetrahydro-1*H*-benzo[de]isoquinolin-1-one (12). This was synthesized according to the original procedure,[45] with minor experimental modifications. The reaction was run in dry glassware under an atmosphere of argon. To a suspension of amide **11** (3.00 g, 10.55 mmol) in 33 mL anhydrous THF at -23 °C (internal temperature), a solution of *n*-BuLi in hexane 2.5M (10.6 mL, 26.5 mmol) was added slowly in portions, over a time period of 1.5 h. The temperature was maintained between -14 °C and -23 °C during the addition. DMF (1.7 mL, 22.58 mmol) was then added in portions over a time period of 2 h. 9 mL 6M aq. HCl was added slowly and the resulting mixture was stirred vigorously for 15 min. The two-phase system was concentrated *in vacuo* to remove most of the THF and hexane. After addition of 40 mL 5M NaOH, the water phase was extracted with EtOAc (3 x 120 mL). The combined organic layers were dried over Na_2SO_4, filtered and concentrated *in vacuo* to afford a yellow sticky solid (3.13 g). The crude product was purified by flash chromatography on silica gel (CH_2Cl_2/ MeOH/Et_3N 9:1:0.1) to give **12** as an off white solid (2.30 g, 74%). IR (neat): 2930, 2868, 1651, 1614, 1594, 1454, 1321, 1262, 1173, 1055, 978, 822, 766 cm^{-1}. ^{1}H NMR (300 MHz, DMSO-*d6*) δ 8.05 (dd, *J* = 7.9, 1.1, 1H), 7.48 (dd, *J* = 7.2, 0.9, 1H), 7.44 (s, 1H), 7.39 (m, 1H), 5.01 – 4.92 (pseudo t, 1H), 3.24 (dd, *J* = 10.4, 1.7, 1H), 3.15 – 3.02 (m, 2H), 2.93 (t, *J* = 6.0, 2H), 2.85 – 2.70 (m, 5H), 1.95 – 1.82 (m, 3H), 1.78

– 1.57 (m, 3H), 1.46 – 1.33 (m, 1H). HRMS (ESI+) calcd for $C_{19}H_{23}N_2O$ $[M+H]^+$ 295.1805, found 295.1796.

(*S*)-2-((1*R*,3*S*,4*R*)-Quinuclidin-3-yl)-2,3,3a,4,5,6-hexahydro-1*H*-benzo[de]isoquinolin-1-one hydrochloride (palonosetron hydrochloride, 1·HCl). This was synthesized according to the original procedure,[45] with some experimental modifications. The reaction was performed in a batch autoclave with a vacuum trap inserted as reaction vessel. To a solution of **12** (2.03 g, 6.9 mmol) in 30 mL glacial acetic acid, was added $HClO_4$ 70% (0.5 mL), $Pd(OH)_2/C$ 20% (40% wet, 838 mg, 0.71 mmol, 11 n/n%) and the autoclave was closed. After flushing the batch hydrogenator three to five times with approximately 10 bar H_2, hydrogen pressure was built up to 25 bar and the reaction mixture was stirred at 70 °C for 24 h. The instrument was allowed to cool down to rt and the pressure released. The reaction mixture was filtered through a plug of celite (pre-washed with MeOH and acetone) and the filter cake washed with MeOH. The solvents were removed under reduced pressure and the resulting mixture was partitioned between 10 mL CH_2Cl_2 and 80 mL 5M NaOH. The water phase was extracted with CH_2Cl_2 (1 x 50 mL and 2 x 20 mL), the combined organic layers dried over Na_2SO_4, filtered and concentrated to afford the crude free base as a white foamy solid (1.82 g). To a solution of the crude free base in 4 mL CH_2Cl_2, was added 4 mL 4M HCl in dioxane. The mixture was stirred for 15 min and concentrated in vacuum to afford the crude hydrochloride as a white solid (2.22 g). The crude HCl salt was co-evaporated once with 10 mL *i*-PrOH and then recrystallized from *i*-PrOH/H_2O (15 mL/0.46 mL, water was added at reflux). Upon cooling, the desired (*S*,*S*)-diastereomer crystallized out. The crystals were filtered, washed with cold mother liquor and 5 mL cold *i*-PrOH to afford **1**·HCl as a white solid (427 mg, 19%). A second recrystallization gave another 178 mg (8%). IR (neat): 2962, 2940, 2923, 2875, 2862, 2461, 1644, 1590, 1408, 1302, 1157, 972, 816, 768 cm^{-1}. ^1H NMR (300 MHz, DMSO-*d6*) δ 10.39 (s, 1H), 7.70 (dd, *J* = 6.9, 1.9, 1H), 7.34 – 7.20 (m, 2H), 4.76 (pseudo t, 1H), 3.77 (dd, *J* = 11.7, 4.7, 1H), 3.65 (br t, *J* = 11.7, 1H), 3.47 (dd, *J* = 13.3, 7.5, 2H), 3.29 – 3.15 (m, 4H), 3.08 – 2.94 (m, 1H), 2.90 – 2.67 (m, 2H), 2.24 – 2.16 (m, 1H), 2.12 – 1.60 (m, 7H), 1.37 – 1.21 (m, 1H). HRMS (ESI+) calcd for $C_{19}H_{25}N_2O$ $[M-HCl+H]^+$ 297.1961, found 297.1967.

(*S*)-2-((1*R*,3*S*,4*R*)-Quinuclidin-3-yl)-2,3,3a,4,5,6-hexahydro-1*H*-benzo[de]isoquinolin-1-one (palonosetron free base, 1). Palonosetron hydrochloride **1**·HCl (196 mg, 0.59 mmol) was partitioned between 15 mL sat. aq. $NaHCO_3$ solution and 30 mL EtOAc. The water phase was extracted with EtOAc (4 x 15 mL). The combined organic layers were dried over Na_2SO_4, filtered and concentrated in vacuum to afford **1** as a foamy sticky solid (168 mg, 96%). ^{1}H NMR (300 MHz, DMSO-*d6*) δ 7.67 (dd, *J* = 5.8, 3.1, 1H), 7.29 – 7.21 (m, 2H), 4.66 – 4.56 (pseudo t, 1H), 3.78 (dd, *J* = 12.0, 4.7, 1H), 3.25 – 3.04 (m, 2H), 3.02 – 2.84 (m, 3H), 2.83 – 2.67 (m, 5H), 2.11 –1.94 (m, 2H), 1.84 – 1.76 (m, 1H), 1.75 – 1.54 (m, 4H), 1.46 – 1.35 (m, 1H), 1.32 –1.24 (m, 1H).

(*S*)-8-Iodo-2-((1*R*,3*S*,4*R*)-quinuclidin-3-yl)-2,3,3a,4,5,6-hexahydro-1*H*-benzo[de]isoquinolin-1-one (13). To a solution of **1** (63 mg, 0.21 mmol) in trifluoromethanesulfonic acid (0.13 mL, 1.47 mmol), was added *N*-iodosuccinimide (287 mg, 1.28 mmol) in portions of 57 mg over a time period of 27 h. After stirring the reaction mixture for a total of 29 h, the reaction was quenched by addition of 10 mL 2M NaOH. The water phase was extracted with CH_2Cl_2 (3 x 10 mL). The combined organic layers were dried over Na_2SO_4, filtered and concentrated in vacuum to afford a brownish solid (71 mg). The crude product was purified by flash chromatography on silica gel (CH_2Cl_2/MeOH/NH_4OH (25% in H_2O) 9:1:0.05) to give iodide **13** as a yellowish solid (37 mg, 41%). IR (neat): 2925, 2862, 1633, 1575, 1429, 1316, 1277, 1170, 1033, 975, 820, 779 cm^{-1}. ^{1}H NMR (300 MHz, DMSO-*d6*) δ 7.94 (d, *J* = 1.6, 1H), 7.66 (d, *J* = 1.7, 1H), 4.66 – 4.54 (pseudo t, 1H), 3.78 (dd, *J* = 12.2, 4.7, 1H), 3.22 – 3.14 (m, 2H), 3.08 – 2.87 (m, 3H), 2.85 – 2.68 (m, 5H), 2.09 – 1.92 (m, 2H), 1.89 – 1.82 (m, 1H), 1.78 – 1.53 (m, 4H), 1.50 – 1.38 (m, 1H), 1.28 – 1.23 (m, 1H). ^{13}C NMR (100 MHz, DMSO-*d6*) δ 163.8, 139.4, 138.7, 137.9, 133.7, 133.1, 92.2, 50.3, 49.56, 46.7, 46.2, 46.0, 33.9, 27.1, 27.0, 25.5, 24.8, 20.9, 20.7. HRMS (ESI+) calcd for $C_{19}H_{24}IN_2O$ $[M+H]^+$ 423.0928, found 423.0919.

(4-Methoxyphenyl)(palonosetron)iodonium ditosylate (14a). To a solution of iodide **13** (37 mg, 0.088 mmol) in CH_2Cl_2/2,2,2-trifluoroethanol 1:1 (0.34 mL), was added *p*-TsOH·H_2O (35 mg, 0.18 mmol). After *p*-TsOH·H_2O was dissolved, dried mCPBA (commercial grade 77%, 23.5 mg, 0.11 mmol) was added

and complete consumption of starting material monitored by TLC. Anisole (11 mL, 0.10 mmol) was added thereafter, the reaction mixture stirred for 6 h at rt and subsequently concentrated in vacuum. The crude product was purified by flash chromatography on alumina (neutral), first using CH_2Cl_2/MeOH 10:0.9, then CH_2Cl_2/MeOH 10:1.4. Iodonium **14** was obtained as a white powder with unknown counterions (26 mg). This material was suspended in 0.5 mL MeCN and *p*-TsOH·H_2O (15.2 mg, 0.08 mmol) added while stirring at rt. The mixture was concentrated in vacuum to afford a yellowish oil (34.5 mg). It was estimated by ^{1}H NMR that the obtained oil contained 63% **14a** and 37% *p*-TsOH by weight (21 mg of **14a**, 27% yield). Alternatively, quantitative counterion exchange was accomplished using a RP-HPLC protocol as previously described.[57] ^{1}H NMR (300 MHz, DMSO-*d6*, hydrogen signals originating from excess *p*-TsOH were omitted for clarity) δ 9.52 (s, 1H), 8.42 (d, *J* = 1.6, 1H), 8.20 (d, *J* = 9.0, 2H), 8.15 (d, *J* = 1.7, 1H), 7.47 (d, *J* = 8.0, 4H), 7.11 (d, *J* = 7.9, 4H), 7.07 (d, *J* = 9.2, 2H), 4.73 (pseudo t, 1H), 3.79 (s, 3H), 3.76 – 3.62 (m, 2H), 3.54 – 3.41 (m, 2H), 3.33 – 3.18 (m, 4H), 3.14 – 3.04 (m, 1H), 2.94 – 2.82 (m, 1H), 2.80 – 2.71 (m, 1H), 2.29 (s, 6H), 2.22 – 2.17 (m, 1H), 2.05 – 1.86 (m, 5H), 1.82 –1.62 (m, 2H), 1.39 – 1.31 (m, 1H). HRMS (ESI+) calcd for $C_{26}H_{30}IN_2O_2$+ $[M\text{-}2TsO\text{-}H]^+$ 529.1346, found 529.1352; calcd for $C_{26}H_{31}IN_2O_2^{2+}$ $[M\text{-}2TsO+H]^{2+}$ 265.0710, found 265.0715.

(4-Methoxyphenyl)(palonosetron)iodonium ditrifluoroacetate (14b). This was synthesized following the procedure for **14a** using iodide **13** (70 mg, 0.17 mmol) in CH_2Cl_2/2,2,2-trifluoroethanol 1:1 (0.68 mL), *p*-TsOH·H_2O (126 mg, 0.66 mmol), dried mCPBA (commercial grade 77%, 81 mg, 0.36 mmol) and anisole (72 mL, 0.66 mmol). The crude product was dissolved in HPLC solvent C (0.1% TFA in water) containing little MeCN and the suspension was filtered. The obtained solution was purified by prep. RP18-HPLC with UV detection at 254 nm, eluting first 2 min with 100% C, then using a gradient from 100% C to 55% D (0.1% TFA in MeCN/H_2O 4:6) in 35 min, 55% D to 100% D in 10 min. The product eluted after 25 min at 32% D. The combined fractions were lyophilized to give **14b** as an off white solid (30 mg, 23%). ^{1}H NMR (300 MHz, $CDCl_3$) δ 12.75 (s, 1H), 8.35 (s, 1H), 7.90 (d, *J* = 8.8, 3H), 6.91 (d, *J* = 8.9, 2H), 4.68 (pseudo t, 1H), 3.82 (s, 3H), 3.89 – 3.75 (m, 1H), 3.68 – 3.56 (m, 3H), 3.38 – 3.21 (m, 4H), 3.13 – 3.01 (m,

1H), 2.95 – 2.70 (m, 2H), 2.36 (s, 1H), 2.20 – 1.88 (m, 6H), 1.79 – 1.63 (m, 1H), 1.32 (dd, *J* = 22.9, 11.1, 1H). ^{13}C NMR (75 MHz, $CDCl_3$) δ 164.4, 162.8, 141.1, 140.2, 138.0, 137.2, 131.9, 131.5, 117.8, 114.8, 104.4, 55.8, 50.9, 50.2, 49.2, 46.0, 45.9, 35.2, 28.2, 25.5, 25.0, 24.0, 21.4, 19.4. ESI-MS *m/z* 529 $[M\text{-}2TFA\text{-}H]^+$.

(2,4,6-Trimethylphenyl)(palonosetron)iodonium ditetrafluoroborate (14c). This was synthesized following the procedure for **14a** using iodide **13** (35 mg, 0.082 mmol) in CH_2Cl_2/2,2,2-trifluoroethanol 1:1 (0.34 mL), *p*-TsOH·H_2O (62 mg, 0.33 mmol), dried mCPBA (commercial grade 77%, 22 mg, 0.10 mmol) and mesitylene (46 mL, 0.33 mmol). The crude iodonium salt was partitioned between 2 mL water and 8 mL EtOAc. The water phase was washed with EtOAc (2 x 8 mL) and subsequently extracted with CH_2Cl_2 (3 x 8 mL). The combined CH_2Cl_2 layers were concentrated *in vacuo* to give the ditosylate salt as a white solid (49 mg, 67%). ^{1}H NMR (300 MHz, DMSO-*d6*) δ 9.50 (s, 1H), 8.11 (d, *J* = 1.6, 1H), 7.89 (d, *J* = 1.5, 1H), 7.46 (d, *J* = 8.0, 4H), 7.23 (s, 2H), 7.11 (d, *J* = 8.0, 4H), 4.69 (pseudo t, 1H), 3.81 – 3.70 (m, 1H), 3.71 – 3.57 (m, 1H), 3.51 – 3.39 (m, 2H), 3.29 – 3.17 (m, 4H), 3.13 – 3.02 (m, 1H), 2.95 – 2.81 (m, 1H), 2.79 – 2.69 (m, 1H), 2.59 (s, 6H), 2.30 (s, 3H), 2.28 (s, 6H), 2.20 – 2.15 (m, 1H), 2.06 – 1.85 (m, 5H), 1.80 – 1.62 (m, 2H), 1.33 – 1.26 (m, 1H). HRMS (ESI+) calcd for $C_{28}H_{34}IN_2O$ $[M\text{-}2TsO\text{-}H]^+$ 541.1710, found 541.1692.

The iodonium ditosylate (49 mg, 0.055 mmol) was partitioned between 6 mL CH_2Cl_2 and 2 mL aq. 1M $NaBF_4$ solution. The aqueous layer was extracted with CH_2Cl_2 (2 x 6 mL). The combined organic layers were extracted with aq. 1M $NaBF_4$ solution (8 mL). The remaining water phase was re-extracted with CH_2Cl_2 (2 x 10 mL). All organic CH_2Cl_2 layers were combined and concentrated *in vacuo* to afford **14c** as a white solid (51 mg, quant.) Integration of tosylate and mesityl signals in the ^{1}H NMR are consistent with almost complete anion exchange (92:8 BF_4^- :TsO^-). ^{1}H NMR (300 MHz, DMSO-*d6*) δ 9.49 (s, 1H), 8.11 (d, *J* = 1.8, 1H), 7.89 (d, *J* = 1.7, 1H), 7.23 (s, 2H), 4.70 (pseudo t, 1H), 3.81 – 3.60 (m, 2H), 3.53 – 3.41 (m, 2H), 3.30 – 3.18 (m, 4H), 3.11 – 3.03 (m, 1H), 2.93 – 2.83 (m, 1H), 2.78 – 2.71 (m, 1H), 2.59 (s, 6H), 2.30 (s, 3H), 2.21 – 2.17 (m, 1H), 2.04 – 1.87 (m, 5H), 1.79 –1.63 (m, 2H), 1.33 – 1.27 (m, 1H).

(*S*)-8-Fluoro-2-((1*R*,3*S*,4*R*)-quinuclidin-3-yl)-2,3,3a,4,5,6-hexahydro-1*H*-benzo[de]isoquinolin-1-one (fluoropalonosetron, 15). A suspension of anisyl iodonium salt **14a** (35 mg, 63 w%, 0.025 mmol) and CsF (11 mg, 0.072 mmol) in 1 mL MeCN (in a capped microwave vial) was stirred at 100 °C for 2 h. The reaction was transferred to an ultrasonic bath, sonicated for 1 h and subsequently stored in the freezer for 72 h. 2 mL acetonitrile was added and the reaction stirred at 100 °C for another 48 h. After allowing the reaction to cool down to rt, the mixture was partitioned between 5 mL CH_2Cl_2 and 2 mL 10% aq. $NaHSO_3$ solution. 5 mL sat. aq. $NaHCO_3$ solution was added and the water phase was extracted with CH_2Cl_2 (2 x 10 mL). The combined organic layers were dried over Na_2SO_4, filtered and concentrated under reduced pressure to afford a yellow solid (12 mg). The yellow solid was dissolved in MeCN with little HPLC solvent C (0.1% TFA in water) and the suspension was filtered. The obtained solution was purified by prep. RP18-HPLC with UV detection at 254 nm, using a gradient of 90% C/10% E (0.1% TFA in MeCN/H_2O 9:1) to 50% E in 30 min, 50% E to 100% E in 10 min. The product eluted after 21 min at 38% E. The combined fractions were lyophilized to give **15** as the trifluoroacetate salt (1.5 mg, 14%).

Fluoropalonosetron **15** was also synthesized using a different method from mesityl iodonium salt **14c**. The reaction was set up in a glove box under nitrogen atmosphere using a microwave vial as reaction vessel. Iodonium salt **14c** (48 mg, 0.067 mmol), copper(II)triflate (12 mg, 0.033 mmol), NaF (4 mg, 0.068 mmol) and 18-crown-6 (7 mg, 0.026 mmol) were dissolved in 0.68 mL DMF. The microwave vial was capped and removed from the glove box. The reaction mixture was stirred at 60 °C for 21 h. DMF was removed *in vacuo* and 5 mL sat. aq. $NaHCO_3$ solution was added. The water phase was extracted with CH_2Cl_2 (3 x 10 mL). The combined organic layers were dried over Na_2SO_4, filtered and concentrated *in vacuo* to afford a yellow solid (21 mg). The yellow solid was dissolved in MeCN with little HPLC solvent C and the suspension was filtered. The obtained solution was purified by prep. RP18-HPLC with UV detection at 254 nm, using a gradient of 90% C/10% E to 50% E in 30 min, 50% E to 100% E in 10 min. The product eluted after 21 min at 38% E. The fractions were lyophilized to give **15** as the trifluoroacetate

salt (3.8 mg, 13%). ^{1}H NMR (300 MHz, $CDCl_3$) δ 13.75 (s, 1H), 7.55 (dd, *J* = 9.0, 2.6, 1H), 6.98 (dd, *J* = 9.1, 2.5, 1H), 4.87 (pseudo t, 1H), 3.77 – 3.65 (m, 1H), 3.63 – 3.53 (m, 3H), 3.39 – 3.21 (m, 4H), 3.07 – 2.92 (m, 1H), 2.88 – 2.77 (m, 2H), 2.42 – 2.33 (m, 1H), 2.19 – 1.89 (m, 6H), 1.80 – 1.73 (m, 1H), 1.39 – 1.29 (m, 1H). ^{13}C NMR (75 MHz, $CDCl_3$) δ 162.4, 138.0, 137.9, 132.7, 132.7, 130.4, 130.3, 119.7, 119.4, 113.5, 113.2, 49.8, 49.6, 49.5, 46.0, 45.9, 34.9, 28.4, 26.3, 25.7, 24.5, 21.8, 19.9 (carbon directly bonded to fluorine, or carbonyl carbon not observed). ^{19}F NMR (376 MHz, DMSO-*d6*) δ -118.87 (t, *J* = 9.1). ESI-MS *m/z* 315 $[M+H]^+$. HRMS (ESI+) calcd for $C_{19}H_{24}FN_2O$ $[M+H]^+$ 315.1867, found 315.1855.

Radiochemistry. *^{11}C-radiolabeling of granisetron*: $[^{11}C]CO_2$ was produced via the $^{14}N(p,\alpha)^{11}C$ nuclear reaction by bombardment of nitrogen gas fortified with 0.5% oxygen using a Cyclone 18/9 cyclotron (18-MeV; IBA, Belgium). After reduction over a supported nickel catalyst to $[^{11}C]CH_4$ and subsequent gas phase iodination, $[^{11}C]CH_3I$ was bubbled through a mixture of desmethyl granisetron precursor **3** (1.0-1.5 mg) and aq. KOH (30 µL, 5 M) in DMF (0.5 mL). The mixture was heated to 90 °C for 3 min. After dilution with 0.1% TFA in water (1.5 mL), the crude product was purified using the semi-preparative HPLC system (product peak at ca. 10 min, Figure S3A). The collected product was diluted with water (10 mL), trapped on a C-18 cartridge (Waters, preconditioned with 5 mL EtOH and 10 mL water), washed with water (5 mL) and eluted with acidified EtOH (0.5 mL, 1% HCl). For formulation of the final product [^{11}C]granisetron ([^{11}C]**2**), PBS (9.5 mL, 0.15 M) was added to give an ethanol concentration of 5%. For quality control, an aliquot of the formulated solution was injected into the analytical HPLC system. The identity of the ^{11}C-labeled product was confirmed by comparison with the retention time of its nonradioactive reference compound granisetron (**2**) and by co-injection with **2** (Figure S4). Specific activity of [^{11}C]granisetron ([^{11}C]**2**) was calculated by comparison of UV peak intensity with a calibration curve of the cold reference compound **2**.

^{18}F-radiolabeling of fluoropalonosetron: No-carrier-added [^{18}F]fluoride was produced via the $^{18}O(p,n)^{18}F$ nuclear reaction by irradiation of isotopically enriched ^{18}O-water in a fixed-energy Cyclone 18/9 cyclotron (IBA). [^{18}F]fluoride was trapped on a light QMA cartridge (Waters), which was

preconditioned with 0.5 M K_2CO_3 (5 mL) and water (5 mL). A 1 mL volume of Kryptofix K_{222}/Cs_2CO_3 solution (Kryptofix K_{222}; 2.5 mg, Cs_2CO_3, 2.6 mg in MeCN (0.7 mL)/water (0.3 mL) was used for the elution of [$^{18}F^-$] from the cartridge. The solvents were evaporated at 100 °C under vacuum in the presence of slight inflow of nitrogen gas, and azeotropic drying was carried out twice with the addition of 0.8 mL acetonitrile each time, to afford dry [^{18}F]CsF/K_{222} complex. A solution of the corresponding iodonium salt precursor **14** (1-2 mg in 0.5 mL dry DMF, 1-2 mg TEMPO) was added to the dried [^{18}F]CsF/K_{222} complex, and the reaction mixture was heated at 140 °C for 12 min and then 8 mL water was added. The reaction mixture was passed through a preconditioned C-18 light cartridge, washed with 5 mL water, eluted the crude product with 1.5 mL acidified ethanol (0.2 M) and followed by 1.5 mL water. Purification was performed by semi-preparative HPLC, with [^{18}F]fluoropalonosetron ([^{18}F]**15**) eluting at about 22 min (Figure S3B). The collected product was diluted with water (8 mL), trapped on a C-18 cartridge (Waters, preconditioned with 5 mL EtOH and 10 mL water), washed with water (5 mL) and eluted with acidified EtOH (1.5 mL, 1% HCl). The ethanol solution was concentrated under vacuum to *ca*. 0.1 mL, then PBS (2 mL, 0.15 M) was added to give an ethanol concentration of 5%. For quality control, an aliquot of the formulated solution was injected into the analytical HPLC system. The identity of the ^{18}F-labeled product [^{18}F]**15** was confirmed by comparison with the retention time of its nonradioactive reference compound fluoropalonosetron **15** and by co-injection with **15** (Figure S5). Specific activity of [^{18}F]fluoropalonosetron ([^{18}F]**15**) was calculated by comparison of UV peak intensity with a calibration curve of the cold reference compound **15**.

Radioligand Competition Binding. All cell culture reagents were obtained from commercial sources and were of the highest obtainable grade. Human 5-HT3A receptor subunit (accession number: P46098) cDNA was obtained from Prof. John Peters (Dundee University, UK) and cloned into pcDNA3.1 (Invitrogen) for expression in HEK 293 cells. HEK 293 cells were maintained on 90 mm tissue culture plates at 37 °C and 7% CO_2 in a humidified atmosphere. They were cultured in DMEM : F12 with Gluta-MAX I media (DMEM/Nutrient Mix F12 (1:1), Invitrogen, Paisley, UK) containing 10 % fetal calf serum.

For radioligand binding studies, cells in 90 mm dishes were transfected using polyethyleneimine (PEI; 25 kDa linear powder; Polysciences Inc., Eppelheim, Germany). 30 mL of PEI (1 mg/mL), 5 µg cDNA and 1 mL DMEM were incubated for 10 min at room temperature, added drop wise to an 80 – 90 % confluent plate, and incubated for 2 – 3 days before harvesting. Transfected HEK 293 cells were scraped into 1 mL of ice-cold HEPES buffer (10 mM, pH 7.4) and frozen. After thawing, they were washed with HEPES buffer, re-suspended, and 50 mg incubated in 0.5 mL HEPES buffer containing the 5-HT_3 receptor antagonist [^{3}H]granisetron ([^{3}H]**2**). For competition binding, reactions were incubated for 24 h at 4 °C with 0.6 nM [^{3}H]granisetron and differing concentrations of competing ligands palonosetron (**1**) and fluoropalonosetron **15**. Non-specific binding was determined using 1 mM quipazine. Reactions were terminated by vacuum filtration using a Brandel cell harvester onto GF/B filters pre-soaked in 0.3% polyethyleneimine. Radioactivity was determined by scintillation counting using a Beckman BCLS6500 (Fullerton, CA, USA). Individual competition binding experiments were analyzed by iterative curve fitting using the following equation in Prism v4.03:

$$y = A_{\text{min}} \frac{A_{\text{max}} - A_{\text{min}}}{1 + 10^{[L] - \log IC_{50}}}$$

where A_{min} is the non-specific binding, A_{max} is the maximum specific binding, [L] is the concentration of competing ligand and IC_{50} is the concentration of competing ligand that blocks half of the specific bound radioligand. For representative dose-inhibition curves see Figure S1. Values were calculated for separate experiments and reported as mean ± SEM.

Determination of log$D_{7.4}$ and *In Vitro* Stability Studies. The partition coefficient D was determined by the shake-flask method as previously described.[68] In brief, *n*-octanol saturated with phosphate buffer pH 7.4 (0.5 mL) and phosphate buffer saturated with n-octanol (0.5 mL) were mixed with either [^{11}C]granisetron ([^{11}C]**2**, 20 µL) or [^{18}F]fluoropalonosetron ([^{18}F]**15**, 10 µL). The samples were shaken for 15 min and then centrifuged at 5000 g for 3 min. Radioactivity in each phase was measured in a gamma

counter (Wizard, PerkinElmer). LogD is expressed as the logarithm of the ratio between the radioactivity concentrations in the *n*-octanol and the phosphate buffer phase.

The tracer stability was examined *in vitro* in rodent plasma (mouse and rat) and human plasma at time points 5, 10, 15 and 20 min. Plasma (400 µL) was incubated with 10 µL of [^{11}C]granisetron ([^{11}C]**2**) solution at 37 °C under shaking. At each time point, an aliquot (100 µL) of the mixture was collected and the reaction stopped with 100 µL ice-cooled MeCN. The samples were centrifuged (3 min, 5000 rpm) and the supernatant collected. Each sample was analyzed by UPLC (Figure S2) using a similar gradient as for HPLC.

Animals. Animal care and experiments were conducted in accordance with Swiss Animal Welfare legislation and approved by the Veterinary Office of the Canton Zürich, Switzerland. Male Wistar rats at 5 weeks of age were purchased from Charles River, Sulzfeld, Germany. Unless otherwise stated, for all *in vivo* experiments animals were anaesthetized with isoflurane in oxygen/air.

***In Vitro* Autoradiography.** Radiotracer binding was evaluated by in vitro autoradiography experiments with 20 µm thick coronal brain cryo-sections of a wild-type mouse (C57BL/6, male) and a rat (Wistar, male) mounted on glass slides (SuperFrost^{TM} Plus, Thermo Scientific, Braunschweig, Germany). Slices were allowed to equilibrate on ice for 10 min before pre-incubated in HEPES buffer (30 mM HEPES, 0.5 mM $MgCl_2$, 110 mM NaCl, 5 mM KCl, 3 mM $CaCl_2$, pH 7.4) supplemented with 0.1% BSA for 10 min at 4°C. Slices were incubated with either 0.6 nM [^{11}C]granisetron ([^{11}C]**2**) or 0.4 nM [^{18}F]fluoropalonosetron ([^{18}F]**15**) in HEPES/0.1% BSA for 15 min or 30 min, respectively, in a humidified chamber at room temperature. For blocking conditions, 1 µM cold palonosetron (**1**) or 1 µM cold quinoline-4-carboxylate **6** was added to the radiotracer solution. The slices were washed for 4 min in HEPES/0.1% BSA buffer, twice for 3 min in HEPES buffer and twice for 5 s in distilled water at 4 °C. The air-dried slides were exposed to a BAS-MS 2025 phosphor imaging plate (Fuji Film, Dielsdorf, Switzerland) for 15 min, scanned in a BAS-5000 bio-imaging reader (Fuji Film, Dielsdorf, Switzerland) and analyzed with the AIDA 4.5 software (Raytest, Sprockhövel, Germany). For histological characterization of the brain

morphology hematoxylin and eosin (HE) (Sigma, St. Louis, MO, USA) staining was applied according to standard protocols. All sections were covered using Eukitt mounting medium (Sigma) and digitized in a slide scanner (Pannoramic 250, Sysmex, Horgen, Switzerland). Specific brain regions were identified according to the anatomical atlas and HE staining.[64]

***In Vivo* PET Imaging and Blocking Studies.** PET scans were performed with a calibrated VISTA eXplore small animal PET/CT scanner (Sedecal, Madrid, Spain). Respiratory rate and temperature were controlled as described previously.[69] In total, 8 Wistar rats (226 - 360 g) were scanned: three brain scans with [^{11}C]granisetron ([^{11}C]**2**) under baseline and one brain scan under blocking conditions, one body [^{11}C]granisetron scan, one brain scan with [^{18}F]fluoropalonosetron ([^{18}F]**15**) under baseline and one under blocking conditions as well as one body [^{18}F]fluoropalonosetron scan. Rats were intravenously injected into the tail vein with 46-53 MBq (brain scan) and 17 MBq (body scan) [^{11}C]granisetron ([^{11}C]**2**) or 30 - 38 MBq (brain scan) and 17 MBq (body scan) [^{18}F]fluoropalonosetron ([^{18}F]**15**). Radiotracer injection and dynamic PET acquisition (list mode) were started simultaneously and PET scan duration was 60 min. Blocking scans were performed by injecting 100 µL cold palonosetron (**1**, 100 µg/kg) intravenously shortly before radiotracer application. At the end of each scan, a CT was recorded for anatomical orientation. PET data were reconstructed in user-defined time frames (2D-OSEM) applying random and scatter corrections. Time-activity curves (TACs) of brain regions were generated with the implemented rat brain region of interest (ROI) template supplied by PMOD biomedical imaging software (3.6, PMOD Technologies Ltd., Zürich, Switzerland). Standardized uptake values (SUV) were calculated as tissue activities (Bq/cm^3), normalized to the injected dose per body weight (Bq/g).

Associated Content

Supporting Information

Proposed mechanism of diaryliodonium salt formation, binding curves for **1** and **15** in competition with radioligand [^{3}H]**2**, detailed procedures to prepare **2** and **6**, copies of ^{1}H, ^{13}C and ^{19}F NMR spectra of **15** and HPLC chromatograms of [^{11}C]**2** and [^{18}F]**15**. This material is available free of charge via the Internet at http://pubs.acs.org.

Abbreviations

5-HT$_3$, 5-hydroxytryptamine (serotonin) type 3 (receptor); DCC, *N*,*N*'-dicyclohexylcarbodiimide; EDC, *N*-(3-dimethylaminopropyl)-*N*'-ethylcarbodiimide; EOB, end of bombardment; GI, gastrointestinal (tract); HE, hematoxylin-eosin; HOBt, 1-hydroxybenztriazole; K_{222}, 4,7,13,16,21,24-hexaoxa-1,10-diazabicyclo[8.8.8]hexacosane (kryptofix); NIS, *N*-iodosuccinimide; NMQ, *N*-methyl quipazine (2-(4-methylpiperazin-1-yl)quinoline); mCPBA, *meta*-chloroperbenzoic acid; RCY, radiochemical yield; SUV, standardized uptake values; TAC, time-activity curve; TEMPO, 2,2,6,6-tetramethylpiperidine 1-oxyl; TFE, 2,2,2-trifluoroethanol; *p*-TsOH, *p*-toluenesulfonic acid;

Author Information

Corresponding Author

*M.L.: phone: +41 31 631 3311; fax +41 31 631 4272; E-mail martin.lochner@dcb.unibe.ch

Present Author Address

[#]F.S.: Philochem AG, Libernstrasse 3, 8112 Otelfingen, Switzerland.

[&]S.M.S.: Wolfson Brain Imaging Centre, Department of Clinical Neurosciences, Addenbrooke's Hospital, University of Cambridge, Cambridge CB2 0QQ, UK.

[⊥]M.L.: Institute of Biochemistry and Molecular Medicine, University of Bern, Bühlstrasse 28, 3012 Bern, Switzerland, martin.lochner@ibmm.unibe.ch

Author Contributions

L.M. planned and coordinated the study, performed and supervised the radiosynthesis, and wrote manuscript. A.M.H. planned and performed *in vitro*/*in vivo* studies and wrote manuscript. P.M.R. performed chemical synthesis. F.S. performed chemical and radiosynthesis. S.M.S. performed ^{11}C-radiolabeling and autoradiography. A.J.T. measured binding affinity of compounds and wrote manuscript. S.D.K., R.S. and S.M.A. discussed experimental data and revised manuscript. M.L. planned and coordinated the study, designed and supervised chemical synthesis, and wrote the manuscript.

Funding Sources

This study was supported by the Swiss National Science Foundation (SNSF professorship PP00P2_123536 and PP00P2_146321 to M.L.) and the British Heart Foundation (PG/13/39/30293 to A.J.T).

Notes

The authors declare no competing financial interest.

Acknowledgments

We thank Prof. Dr. Wolf-D. Woggon and Prof. Dr. Antoinette Chougnet for synthesizing **6**, the analytical services form the Department of Chemistry and Biochemistry, University of Bern, for measuring NMR and MS spectra, Mr. Bruno Mancosu for technical support with ^{11}C-radiolabeling, Mr. Stjepko Čermak for help with C^{11}-autoradiography and Mrs. Claudia Keller for animal care and performing PET/CT scans.

References

(1) Thompson, A. J. (2013) Recent developments in 5-HT_3 receptor pharmacology. *Trends Pharmacol. Sci. 34*, 100-109.

(2) Wong, E. H., Clark, R., Leung, E., Loury, D., Bonhaus, D. W., Jakeman, L., Parnes, H., Whiting, R. L., and Eglen, R. M. (1995) The interaction of RS 25259-197, a potent and selective antagonist, with 5-HT_3 receptors, *in vitro*. *Br. J. Pharmacol. 114*, 851-859.

(3) Rojas, C., Stathis, M., Thomas, A. G., Massuda, E. B., Alt, J., Zhang, J., Rubenstein, E., Sebastiani, S., Cantoreggi, S., Snyder, S. H., and Slusher, B. (2008) Palonosetron exhibits unique molecular interactions with the 5-HT_3 receptor. *Anesth. Analg. 107*, 469-478.

(4) Del Cadia, M., De Rienzo, F., Weston, D. A., Thompson, A. J., Menziani, M. C., and Lummis, S. C. R. (2013) Exploring a potential palonosetron allosteric binding site in the 5-HT_3 receptor. *Bioorg. Med. Chem. 21*, 7523-7528.

(5) Hothersall, J. D., Moffat, C., and Connolly, C. N. (2013) Prolonged inhibition of 5-HT_3 receptors by palonosetron results from surface receptor inhibition rather than inducing receptor internalization. *Br. J. Pharmacol. 169*, 1252-1262.

(6) Lummis, S. C. R., and Thompson, A. J. (2013) Agonists and antagonists induce different palonosetron dissociation rates in 5-HT_3A and 5-HT_3AB receptors. *Neuropharmacology 73*, 241-246.

(7) Costall, B., and Naylor, R. J. (1992) Neuropharmacology of emesis in relation to clinical response. *Br. J. Cancer Suppl. 19*, S2-S8.

(8) Hornby, P. J. (2001) Central neurocircuitry associated with emesis. *Am. J. Med. 111*, 106-112.

(9) Minami, M., Endo, T., Hirafuji, M., Hamaue, N., Liu, Y., Hiroshige, T., Nemoto, M., Saito, H., and Yoshioka, M. (2003) Pharmacological aspects of anticancer drug-induced emesis with emphasis on serotonin release and vagal nerve activity. *Pharmacol. Ther. 99*, 149-165.

(10) Machu, T. K. (2011) Therapeutics of 5-HT_3 receptor antagonists: current uses and future directions. *Pharmacol. Ther. 130*, 338-347.

(11) Walstab, J., Rappold, G., and Niesler, B. (2010) 5-HT_3 receptors: role in disease and target of drugs. *Pharmacol. Ther. 128*, 146-169.

(12) Bétry, C., Etiévant, A., Oosterhof, C., Ebert, B., Sanchez, C., and Haddjeri, N. (2011) Role of 5-HT_3 receptors in the antidepressant response. *Pharmaceuticals 4*, 603.

(13) Kilpatrick, G. J., Jones, B. J., and Tyers, M. B. (1987) Identification and distribution of 5-HT_3 receptors in rat brain using radioligand binding. *Nature 330*, 746-748.

(14) Glaum, S. R., Brooks, P. A., Spyer, K. M., and Miller, R. J. (1992) 5-Hydroxytryptamine-3 receptors modulate synaptic activity in the rat nucleus tractus solitarius in vitro. *Brain Res. 589*, 62-68.

(15) Wang, Y., Ramage, A. G., and Jordan, D. (1998) Presynaptic 5-HT_3 receptors evoke an excitatory response in dorsal vagal preganglionic neurones in anaesthetized rats. *J. Physiol. 509*, 683-694.

(16) Miquel, M. C., Emerit, M. B., Nosjean, A., Simon, A., Rumajogee, P., Brisorgueil, M. J., Doucet, E., Hamon, M., and Vergé, D. (2002) Differential subcellular localization of the 5-HT_3-A_s receptor subunit in the rat central nervous system. *Eur. J. Neurosci. 15*, 449-457.

(17) Jeggo, R. D., Kellett, D. O., Wang, Y., Ramage, A. G., and Jordan, D. (2005) The role of central 5-HT_3 receptors in vagal reflex inputs to neurones in the nucleus tractus solitarius of anaesthetized rats. *J. Physiol. 566*, 939-953.

(18) Barnes, N. M., Hales, T. G., Lummis, S. C. R., and Peters, J. A. (2009) The 5-HT_3 receptor – the relationship between structure and function. *Neuropharmacology 56*, 273-284.

(19) Fozard, J. R. (1984) Neuronal 5-HT receptors in the periphery. *Neuropharmacology 23*, 1473-1486.

(20) Richardson, B. P., Engel, G., Donatsch, P., and Stadler, P. A. (1985) Identification of serotonin M-receptor subtypes and their specific blockade by a new class of drugs. *Nature 316*, 126-131.

(21) Andrews, P. L., and Hawthorn, J. (1988) The neurophysiology of vomiting. *Baillieres Clin. Gastroenterol. 2*, 141-168.

(22) Sakurai-Yamashita, Y., Yamashita, K., Yoshimura, M., and Taniyama, K. (1999) Differential localization of 5-hydroxytryptamine$_3$ and 5-hydroxytryptamine$_4$ receptors in the human rectum. *Life Sci. 66*, 31-34.

(23) Michel, K., Zeller, F., Langer, R., Nekarda, H., Kruger, D., Dover, T. J., Brady, C. A., Barnes, N. M., and Schemann, M. (2005) Serotonin excites neurons in the human submucous plexus via 5-HT$_3$ receptors. *Gastroenterology 128*, 1317-1326.

(24) Böttner, M., Bär, F., Von Koschitzky, H., Tafazzoli, K., Roblick, U. J., Bruch, H. p., and Wedel, T. (2010) Laser microdissection as a new tool to investigate site-specific gene expression in enteric ganglia of the human intestine. *Neurogastroenterol. Motil. 22*, 168-172.

(25) Fiebich, B. L., Akundi, R. S., Seidel, M., Geyer, V., Haus, U., Muller, W., Stratz, T., and Candelario-Jalil, E. (2004) Expression of 5-HT$_3$A receptors in cells of the immune system. *Scand. J. Rheumatol. Suppl. 119*, 9-11.

(26) Jack, T., Simonin, J., Ruepp, M. D., Thompson, A. J., Gertsch, J., and Lochner, M. (2015) Characterizing new fluorescent tools for studying 5-HT$_3$ receptor pharmacology. *Neuropharmacology 90*, 63-73.

(27) Smith, D. F., and Jakobsen, S. (2013) Molecular neurobiology of depression: recent PET findings on the elusive correlation with symptom severity. *Front. Psychiatry 4*.

(28) Barré, L., Debruyne, D., Lasne, M. C., Gourand, F., Bonvento, G., Camsonne, R., Moulin, M., and Baron, J. C. (1992) Synthesis and regional rat brain distribution of [^{11}C]MDL 72222: a 5HT$_3$ receptor antagonist. *Appl. Radiat. Isot. 43*, 509-516.

(29) Camsonne, R., Barré, L., Petit-Taboué, M.-C., Travére, J. M., Jones, R., Debruyne, D., Moulin, M. A., MacKenzie, E. T., and Baron, J. C. (1993) Positron emission tomographic studies of [^{11}C]MDL 72222, a potential 5-HT$_3$ receptor radioligand: distribution, kinetics and binding in the brain of the baboon. *Neuropharmacology 32*, 65-71.

(30) Rajagopal, S., Diksic, M., Francis, B., Swain, C. J., and Burns, H. D. (1992) Synthesis of a ^{11}C-labeled novel, quinuclidine based ligand for the 5-HT$_3$ receptor. *Appl. Radiat. Isot. 43*, 1369-1373.

(31) Ishiwata, K., Ishii, K., Ishii, S.-I., and Senda, M. (1995) Synthesis of 5-HT$_3$ receptor antagonists, [^{11}C]Y-25130 and [^{11}C]YM060. *Appl. Radiat. Isot. 46*, 907-910.

(32) Ishiwata, K., Saito, N., Yanagawa, K., Furuta, R., Ishii, S.-I., Kiyosawa, M., Homma, Y., Ishii, K., Suzuki, F., and Senda, M. (1996) Synthesis and evaluation of 5-HT$_3$ receptor antagonist [^{11}C]KF17643. *Nucl. Med. Biol. 23*, 285-290.

(33) Vandersteene, I., Audenaert, K., Slegers, G., and Dierckx, R. (1998) Synthesis of [^{11}C]granisetron, a possible positron emission tomography ligand for 5-HT$_3$ receptor studies. *J. Labelled Compd. Radiopharm. 41*, 171-180.

(34) Thorell, J.-O., Stone-Elander, S., Eriksson, L., and Ingvar, M. (1997) *N*-methylquipazine: Carbon-11 labelling of the 5-HT$_3$ agonist and *in vivo* evaluation of its biodistribution using PET. *Nucl. Med. Biol. 24*, 405-412.

(35) Guillouet, S., Barré, L., Gourand, F., Lasne, M. C., and Rault, S. (1996) Synthesis of [^{11}C]-S21007 a novel 5HT$_3$ partial agonist as a potential tracer for PET studies. *J. Labelled Compd. Radiopharm. 38*, 367-371.

(36) Besret, L., Dauphin, F., Guillouet, S., Dhilly, M., Gourand, F., Blaizot, X., Young, A. R., Petit-Taboué, M. C., Mickala, P., Barbelivien, A., Rault, S., Barré, L., and Baron, J. C. (1997) [^{11}C]S21007, a putative partial agonist for 5-HT_3 receptors PET studies. Rat and primate *in vivo* biological evaluation. *Life Sci. 62*, 115-129.

(37) Katounina, T., Besret, L., Dhilly, M., Petit-Taboué, M.-C., Barbelivien, A., Baron, J.-C., Dauphin, F., and Barré, L. (1998) Synthesis and biological investigations of [^{18}F]MR18445, a 5-HT_3 receptor partial agonist. *Bioorg. Med. Chem. 6*, 789-795.

(38) Gao, M., Wang, M., Hutchins, G. D., and Zheng, Q.-H. (2008) Synthesis of new carbon-11 labeled benzoxazole derivatives for PET imaging of 5-HT_3 receptor. *Eur. J. Med. Chem. 43*, 1570-1574.

(39) Pithia, N. K., Liang, C., Pan, X.-Z., Pan, M.-L., and Mukherjee, J. (2016) Synthesis and evaluation of (*S*)-[^{18}F]fesetron in the rat brain as a potential PET imaging agent for serotonin 5-HT_3 receptors. *Bioorg. Med. Chem. Lett. 26*, 1919-1924.

(40) Vernekar, S. K. V., Hallaq, H. Y., Clarkson, G., Thompson, A. J., Silvestri, L., Lummis, S. C. R., and Lochner, M. (2010) Toward biophysical probes for the 5-HT_3 receptor: structure−activity relationship study of granisetron derivatives. *J. Med. Chem. 53*, 2324-2328.

(41) Dalmases, B. P., and Puig, T. S. (2003) High-yield process for preparing granisetron and its acid-addition salts. WO2003/080606 A1.

(42) Thompson, A. J., and Lochner, M. (unpublished experiments).

(43) Cappelli, A., Gallelli, A., Manini, M., Anzini, M., Mennuni, L., Makovec, F., Menziani, M. C., Alcaro, S., Ortuso, F., and Vomero, S. (2005) Further studies on the interaction of the 5-hydroxytryptamine$_3$ (5-HT_3) receptor with arylpiperazine ligands. Development of a new 5-HT_3 receptor ligand showing potent acetylcholinesterase inhibitory properties. *J. Med. Chem. 48*, 3564-3575.

(44) Dulla, B., Wan, B., Franzblau, S. G., Kapavarapu, R., Reiser, O., Iqbal, J., and Pal, M. (2012) Construction and functionalization of fused pyridine ring leading to novel compounds as potential antitubercular agents. *Bioorg. Med. Chem. Lett. 22*, 4629-4635.

(45) Clark, R. D., Miller, A. B., Berger, J., Repke, D. B., Weinhardt, K. K., Kowalczyk, B. A., Eglen, R. M., Bonhaus, D. W., and Lee, C. H. (1993) 2-(Quinuclidin-3-yl)pyrido[4,3-*b*]indol-1-ones and isoquinolin-1-ones. Potent conformationally restricted 5-HT_3 receptor antagonists. *J. Med. Chem. 36*, 2645-2657.

(46) Chatterjee, S., Rawat, A. S., Pawar, A. V., Rajanikanth, J., and P., V. (2011) Process for the preparation of substantially pure palonosetron and its acid salts. US2001/0021778 A1.

(47) Pike, V. W., and Aigbirhio, F. I. (1995) Reactions of cyclotron-produced [^{18}F]fluoride with diaryliodonium salts-a novel single-step route to no-carrier-added [^{18}]fluoroarenes. *J. Chem. Soc., Chem. Commun.*, 2215-2216.

(48) Rotstein, B. H., Stephenson, N. A., Vasdev, N., and Liang, S. H. (2014) Spirocyclic hypervalent iodine(III)-mediated radiofluorination of non-activated and hindered aromatics. *Nat. Commun. 5*, 4365.

(49) Shah, A., W. Pike, V., and A. Widdowson, D. (1998) The synthesis of [^{18}F]fluoroarenes from the reaction of cyclotron-produced [^{18}F]fluoride ion with diaryliodonium salts. *J. Chem. Soc., Perkin Trans. 1*, 2043-2046.

(50) Yusubov, M. S., Maskaev, A. V., and Zhdankin, V. V. (2011) Iodonium salts in organic synthesis. *Arkivoc 2011*, 370-409.

(51) Yusubov, M. S., Svitich, D. Y., Larkina, M. S., and Zhdankin, V. V. (2013) Applications of iodonium salts and iodonium ylides as precursors for nucleophilic fluorination in positron emission tomography. *Arkivoc 2013*, 364-395.

(52) Carroll, M. A., Jones, C., and Tang, S.-L. (2007) Fluoridation of 2-thienyliodonium salts. *J. Labelled Compd. Radiopharm. 50*, 450-451.

(53) Olah, G. A., Wang, Q., Sandford, G., and Surya Prakash, G. K. (1993) Synthetic methods and reactions. 181. Iodination of deactivated aromatics with *N*-iodosuccinimide in trifluoromethanesulfonic acid (NIS-CF_3SO_3H) via *in situ* generated superelectrophilic iodine(I) trifluoromethanesulfonate. *J. Org. Chem. 58*, 3194-3195.

(54) Bielawski, M., and Olofsson, B. (2007) High-yielding one-pot synthesis of diaryliodonium triflates from arenes and iodine or aryl iodides. *Chem. Commun.*, 2521-2523.

(55) Zhu, M., Jalalian, N., and Olofsson, B. (2008) One-pot synthesis of diaryliodonium salts using toluenesulfonic acid: A fast entry to electron-rich diaryliodonium tosylates and triflates. *Synlett*, 592-596.

(56) Ross, T. L., Ermert, J., Hocke, C., and Coenen, H. H. (2007) Nucleophilic ^{18}F-fluorination of heteroaromatic iodonium salts with no-carrier-added [^{18}F]fluoride. *J. Am. Chem. Soc. 129*, 8018-8025.

(57) Selivanova, S. V., Stellfeld, T., Heinrich, T. K., Müller, A., Krämer, S. D., Schubiger, P. A., Schibli, R., Ametamey, S. M., Vos, B., Meding, J., Bauser, M., Hütter, J., and Dinkelborg, L. M. (2013) Design, synthesis, and initial evaluation of a high affinity positron emission tomography probe for imaging matrix metalloproteinases 2 and 9. *J. Med. Chem. 56*, 4912-4920.

(58) Lee, B. C., Lee, K. C., Lee, H., Mach, R. H., and Katzenellenbogen, J. A. (2007) Strategies for the labeling of halogen-substituted peroxisome proliferator-activated receptor γ ligands: Potential positron emission tomography and single photon emission computed tomography imaging agents. *Bioconjugate Chem. 18*, 514-523.

(59) Ichiishi, N., Canty, A. J., Yates, B. F., and Sanford, M. S. (2013) Cu-catalyzed fluorination of diaryliodonium salts with KF. *Org. Lett. 15*, 5134-5137.

(60) Okuyama, T., Takino, T., Sueda, T., and Ochiai, M. (1995) Solvolysis of cyclohexenyliodonium salt, a new precursor for the vinyl cation: Remarkable nucleofugality of the phenyliodonio group and evidence for internal return from an intimate ion-molecule pair. *J. Am. Chem. Soc. 117*, 3360-3367.

(61) Ory, D., Van den Brande, J., de Groot, T., Serdons, K., Bex, M., Declercq, L., Cleeren, F., Ooms, M., Van Laere, K., Verbruggen, A., and Bormans, G. (2015) Retention of [^{18}F]fluoride on reversed phase HPLC columns. *J. Pharm. Biomed. Anal. 111*, 209-214.

(62) Wiberg, E., Wiberg, N., and Holleman, A. F. (2001) *Inorganic Chemistry*, 1st ed., Academic Press, San Diego.

(63) Kilpatrick, G. J., Jones, B. J., and Tyers, M. B. (1989) Binding of the 5-HT$_3$ ligand, [^{3}H]GR65630, to rat area postrema, vagus nerve and the brains of several species. *Eur. J. Pharmacol. 159*, 157-164.

(64) Paxinos, G., and Watson, C. (2004) *The rat brain in stereotaxic coordinates*, 6th ed., Elsevier Academic, London.

(65) Dumas, N., Moulin-Sallanon, M., Ginovart, N., Tournier, B. B., Suzanne, P., Cailly, T., Fabis, F., Rault, S., Charnay, Y., and Millet, P. (2014) Small-animal single-photon emission computed tomographic imaging of the brain serotoninergic systems in wild-type and *Mdr1a* knockout rats. *Mol. Imaging 13*.

(66) Kilpatrick, G. J., Jones, B. J., and Tyers, M. B. (1988) The distribution of specific binding of the 5-HT$_3$ receptor ligand [^{3}H]GR65630 in rat brain using quantitative autoradiography. *Neurosci. Lett. 94*, 156-160.

(67) Pajouhesh, H., and Lenz, G. R. (2005) Medicinal chemical properties of successful central nervous system drugs. *NeuroRx 2*, 541-553.

(68) Wilson, A. A., Jin, L., Garcia, A., DaSilva, J. N., and Houle, S. (2001) An admonition when measuring the lipophilicity of radiotracers using counting techniques. *Appl. Radiat. Isot. 54*, 203-208.

(69) Müller Herde, A., Keller, C., Milicevic Sephton, S., Mu, L., Schibli, R., Ametamey, S. M., and Krämer, S. D. (2015) Quantitative positron emission tomography of mGluR5 in rat brain with [^{18}F]PSS232 at minimal invasiveness and reduced model complexity. *J. Neurochem. 133*, 330-342.

Table of Contents Graphic

For Table of Contents Use Only